Effects of Polymerization Conditions and Imidization Methods on Performance of Crosslinkable Polymer Membrane for CO_2/CH_4 Separation

A Thesis
Presented to
The Academic Faculty

by

Danny Jinsoo Kim

In Partial Fulfillment
Of the Requirements for the Degree
Master of Science in the
School of Chemical & Biomolecular Engineering

Georgia Institute of Technology

August, 2013

Effects of Polymerization Conditions and Imidization Methods on Performance of Crosslinkable Polymer Membrane for CO_2/CH_4 Separation

Approved by:

Dr. William Koros, Advisor
School of Chemical &
Biomolecular Engineering
Georgia Institute of Technology

Dr. Tom Fuller
School of Chemical &
Biomolecular Engineering
Georgia Institute of Technology

Dr. Krista Walton
School of Chemical &
Biomolecular Engineering
Company
Georgia Institute of Technology

Dr. Stephen Miller
Chevron Fellow
Chevron Energy Technology

Date Approved: March, 2013

Dedicated To

My family and Yoohwa

ACKNOWLEDGEMENTS

Above all, I would like to express my deepest gratitude to my advisor, Dr. Koros, for his excellent guidance, helpful suggestion, and infinite patience over the past two years. I consider myself extremely fortunate to have him as my mentor as he has been instrumental in my growth as a person and a professional. I would also like to thank my committee members, Dr. Tom Fuller, Dr. Krista Walton, and Dr. Stephen Miller for their time and valuable efforts. Especially, Dr. Stephen Miller from Chevron has visited Georgia Tech every quarter and shared ideas full of insight. . From Chevron, Dr. Hussain, Dr. Wind and Dr. Chin also provided valuable technical feedback. I greatly appreciate the generous funding support from Chevron as well.

I would like to acknowledge the whole of the Koros group members. Special credits go to: Brian Kraftschik, Dr. Justin Vaughn, Steven Burgess, Vinod Babu and Dr. Jong Lee for the valuable discussion and personal technical training, Chen Zhang and Dr. Kuang Zhang for the system introduction, Dr. Wulin Qiu for the polymer synthesis.

I must thank to my family for their unconditional and endless support from the other end of world. The friends I've made in Atlanta have helped me stay motivated throughout my Ph.D. study.

None of this would have been possible without endless patience, encouragement, and understanding of my girlfriend Yoohwa Seong (Tiffany). She always willingly came to school with me on weekend and supported me whenever I have a deadline approaching. I absolutely cannot imagine completing my work without her.

TABLE OF CONTENTS

ACKNOWLEDGEMENTS iv

LIST OF TABLES ix

LIST OF FIGURES xx

SUMMARY ..... **iv**

CHAPTER 1 INTRODUCTION **1**

1.1 Natural gas overview **1**

1.2 Natural gas separation membranes **2**

1.3 Research objectives **4**

1.4Thesis organization **5**

1.5 References **5**

CHAPTER 2 BACKGROUND AND THEORY **6**

2.1 Gas transport in polymer membranes **6**

2.1.1 General transport theory 6

2.1.2 Characterization of dense film membranes 8

2.1.3 Plasticization of polymer membranes 9

2.1.4 Physical aging 11

2.2 Copolymer and transamidation **12**

2.3 References **14**

CHAPTER 3 MATERIALS AND PROCEDURES **17**

3.1 Materials **17**

3.1.1 Polyamic acid synthesis 17

3.1.2 Imidization 18

3.1.3 Monoesterification 19

3.2 Dense film membrane preparation **20**

3.3 Dense film characterization techniques **21**

3.3.1 Pure gas permeation 21
3.3.2 Mixed gas permeation 22
3.3.3 Gel Permeation Chromatography (GPC) 23
3.3.4 Fourier-Transform Infrared spectroscopy (FTIR) 23
3.3.5 Thermo Gravimetric analysis (TGA) 23
3.3.6 X-Ray diffraction (XRD) 23
3.3.7 Differential Scanning Calorimetry (DSC) 24
3.3.8 Dynamic Mechanical Analysis (DMA) 24
3.3.9 Nuclear Magnetic Resonance spectroscopy (NMR) 24
3.3.10 Gel fraction test 25
3.4 References 25

CHAPTER 4 OPTIMIZATION OF POLYMERIZATION CONDITIONS FOR THE PERFORMANCE OF CHEMICALLY IMIDIZED PDMC 27
4.1 Introduction 27
4.2 Effect of polymerization conditions on molecular weight of *chemically imidized* PDMC 29
4.3 Effect of polymerization conditions on transport properties of *chemically imidized* PDMC 31
4.4 Effect of polymerization conditions on plasticization suppression 34
4.5 Gel fraction test 35
4.6 Conclusions 35
4.7 References 36

CHAPTER 5 PERFORMANCE OF THERMALLY IMIDIZED PDMC 37
5.1Introduction 37
5.2 Gas permeation 37
5.2.1 Pure gas permeation 37
5.2.2 Mixed gas permeation 39
5.3 FTIR analysis of imidization methods 39
5.4 NMR analysis of imidization methods 43

5.5 TGA analysis of imidization methods 47

5.6 DSC analysis of imidization methods 52

5.7 DMA analysis of imidization methods 54

5.8 XRD analysis of imidization methods 55

5.9 Gel fraction test and dissolution test 58

5.10 Conclusions 60

5.11 References 60

CHAPTER 6 EFFECTS OF AGGRESSIVE FEEDS ON HIGH PERFORMANCE ESTER-CROSSLINKED DENSE FILM 63

6.1 Introduction 63

6.2 Effects of high CO_2 partial pressures 63

6.3 Effects of operating temperatures 65

6.4 Stability of dense films under high feed pressures 68

6.5 Conclusions 69

6.6 References 69

CHAPTER 7 CONCLUSION AND RECOMMENDATION FOR FUTURE WORK ... 70

7.1 Summary 70

7.2 Conclusions 70

7.2.1 Optimization of polymerization conditions of chemically imidized PDMC 70

7.2.2 Significantly improved separation performance thermally imidized PDMC 70

7.2.3 Characterization of ester-crosslinked dense film under aggressive gas feed 71

7.3 Recommendations for Future Work 71

7.3.1 Sorption test on chemically imidized PDMC and thermally imidized PDMC 71

7.3.2 Extension to composite hollow fiber 70

7.3.3 Aggressive feed conditions 72

7.4 References **73**

Appendix A: CHEMICAL IMIDIZATION **74**

Appendix B: THERMAL IMIDIZATION **75**

Appendix C: MONOESTERIFICATION **76**

LIST OF TALBES

Table 1.1 Natural gas pipeline specifications in the U.S. [3] 2

Table 2.1: Kinetic diameters and critical temperatures for practical gases [7] 9

Table 4.1: Polymerization conditions. The italic numbers refer to state number identifiers 29

Table 4.2: Gel fraction of *chemically imidized* PDMC……...35

Table 5.1: Pure gas permeation data of this work and literature [1-3] 37

Table 5.2: Source of three peaks 3670cm^{-1}, 2900cm^{-1} and 1067cm^{-1} [6]..... 42

Table 5.3: T_g data of this study and literatures [13-15] 52

Table 5.4: Gel fraction of *chemically imidized* PDMC and *thermally imidized* PDMC 59

LIST OF FIGURES

Figure 1.1: World Energy Consumption by fuel [1] 1

Figure 1.2: Robeson's 2008 upper bound showing the tradeoff between permeability and selectivity for polymer membranes [4] 3

Figure 2.1: Schematics of diffusion through a polymer via transient gap formation 7

Figure 2.2: Schematics of permeability increase and selectivity decrease due to membrane plasticization 10

Figure 2.3: Schematic illustration of the specific volume vs. T for a glassy polymer 11

Figure 2.4: Schematic illustration of random copolymer and block copolymer including A and B where A is 6FDA-DAM and B is 6FDA-DABA in this work 12

Figure 2.5: Three kinds of transamidation: aminolysis, acidolysis, and amidolysis [22] 13

Figure 3.1: Reaction scheme for polycondensation reaction from monomer to 6FDA-DAM: DABA (3:2) polyamic acid 17

Figure 3.2: Reaction scheme for imidization from polyamic acid to 6FDA-DAM:DABA (3:2) polyimide 19

Figure 3.3: Reaction scheme for monoesterification of 6FDA-DAM:DABA (3:2) with 1,3-propanediol to form PDMC 20

Figure 3.4: Schematic illustration of dense film membrane casting 21

Figure 3.5: Gas permeation system for dense film [8] 21

Figure 4.1: Flowchart of possible optimization of *chemically imidized* PDMC related to different potentially controlling factors 29

Figure 4.2: Polymerization temperature impact on Molecular weight of 6FDA-DAM:DABA (3:2) 30

Figure 4.3: Polymerization time impact on Molecular weight of 6FDA-DAM:DABA (3:2) 31

Figure 4.4: Polymerization temperature impact on CO_2 permeability 31

Figure 4.5: Polymerization time impact on CO_2 permeability 32

Figure 4.6: Polymerization temperature impact on CO_2/CH_4 selectivity 33

Figure 4.7: Polymerization time impact on CO_2/CH_4 selectivity..... 33

Figure 4.8: Plasticization suppression of *chemically imidized* PDMC. Test conditions: Pure CO_2, CH_4 at 35℃ 34

Figure 5.1: Plasticization suppression of *chemically imidized* PDMC in this work, thermally imidized PDMC in this work, and Hillock's *thermally imidized* PDMC. Test conditions: Pure CO_2, CH_4 at 35℃. [3] 38

Figure 5.2: FTIR results of chemically imidized 6FDA-DAM:DABA(3:2) and *thermally imidized* 6FDA-DAM:DABA (3:2)..... 40

Figure 5.3: FTIR results of chemically imidized uncrosslinked PDMC and *thermally imidized* uncrosslinked PDMC [above] and chemically imidized crosslinked PDMC and *thermally imidized* crosslinked PDMC [below]..... 41

Figure 5.4: ^{1}H NMR results of *chemically imidized* 6FDA-DAM:DABA (3:2) and *thermally imidized* 6FDA-DAM:DABA (3:2) 43

Figure 5.5: ^{1}H NMR results of *chemically imidized* PDMC and *thermally imidized* PDMC..... 44

Figure 5.6: Partial ring opening of PDMC [9] 45

Figure 5.7: Comparison of NMR results of chemically imidized PDMC #3, #6, and #10 46

Figure 5.8: TGA traces of chemically imidized 6FDA-DAM:DABA (3:2) and *thermally imidized* 6FDA-DAM:DABA (3:2)..... 47

Figure 5.9: A decarboxylation mechanism 48

Figure 5.10: a) Thermally imidized 6FDA-DAM:DABA(3:2) with less flexible DABA moieties b) Chemically imidized 6FDA-DAM:DABA(3:2) with more flexible DABA domain 49

Figure 5.11: TGA traces of uncrosslinked PDMC (above) and crosslinked PDMC (below). 50

Figure 5.12: T_g of 6FDA-DAM, 6FDA-mPDA and 6FDA-DABA [7]. 53

Figure 5.13: DSC results of *chemically imidized* 6FDA-DAM:DABA (3:2) and *thermally imidized* 6FDA-DAM:DABA (3:2). Tg of *chemically imidized* PDMC: 383℃, Tg of *thermally imidized* PDMC: 388℃ 53

Figure 5.14: DSC results of *chemically imidized* PDMC and *thermally imidized* PDMC. Tg of *chemically imidized* PDMC: 367℃, Tg of *thermally imidized* PDMC: 378℃ 54

Figure 5.15: DMA results of *chemically imidized* PDMC and *thermally imidized* PDMC. T_g of *chemically imidized* PDMC: 378℃, T_g of *thermally imidized* PDMC: 390℃ 54

Figure 5.16: XRD results of *chemically imidized* 6FDA-DAM:DABA (3:2) and *thermally imidized* 6FDA-DAM:DABA (3:2) 55

Figure 5.17: XRD results of *chemically imidized* PDMC and *thermally imidized* PDMC 56

Figure 5.18: XRD results of chemically imidized PDMC #3, #6, and #10 57

Figure 5.19: XRD results of chemically imidized PDMC #4, #5, and #6 58

Figure 5.20: Dissolution test (Left: *chemically imidized* PDMC dissolved in NMP, Right: *thermally imidized* PDMC dissolved in NMP) 59

Figure 6.1: CO_2 permeability of crosslinked dense film at elevated feed pressures from this work. Permeability calculated by using fugacity. Test conditions: 50/50 CO_2/CH_4, mixed gas at 35°C 63

Figure 6.2: CO_2/CH_4 selectivity of crosslinked dense film at elevated feed pressures from this work. Selectivity calculated by using fugacity. Test conditions: 50/50 CO_2/CH_4, mixed gas at 35°C 64

Figure 6.3: Transport properties of c*hemically imidized* PDMC at different operating temperatures. Transport properties were calculated using fugacity at corresponding temperatures and pressures. Test conditions: 50/50 CO_2/CH_4 mixed gas at 22℃, 35℃, and 50℃ up to total feed 800psi 65

Figure 6.4: Transport properties of *thermally imidized* PDMC at different operating temperatures. Transport properties were calculated using fugacity at corresponding temperatures and pressures. Test conditions: 50/50 CO_2/CH_4 mixed gas at 22℃, 35℃, and 50℃ up to total feed 800psi 66

Figure 6.5: Plotting log P vs. 1000/T 67

Figure 6.6: Stability of dense films under high feed pressures. Permeabilities and selectivities were calculated using fugacity at corresponding temperatures and pressures. Test conditions: 600psi, 50/50 CO_2/CH_4 mixed gas at 35℃ 68

Figure 7.1: Scanning electron microscope (SEM) images showing the cross-section of a crosslinked PDMC/CA composite hollow fiber [1] 72

Figure A.1: Chemical imidization reaction of polyamic acid with beta picoline and acetate anhydride below room temperature [1] 74

Figure B.1: Thermal imidization reaction of polyamic acid with ODCB at 190℃ [1] 75

Figure C.1: Monoesterification reaction of 6FDA-DAM: DABA (3:2) polyimide with 1,3-propanediol [1] 76

Figure C.2: Schematic showing the set-up for monoesterification reaction [1] 77

SUMMARY

Natural gas feeds often contain contaminants such as CO_2, H_2S, H_2O, and small hydrocarbons. Carbon dioxide is a major contaminant reducing the heating value of the gas and causing pipeline corrosion, so CO_2 level should be lowered to below 2% to meet the United States pipeline specifications. Membrane separation technology can be advantageous over cryogenic distillation and amine adsorption in terms of cost and efficiency. The key hurdle to overcome in polymeric membrane separation technology is improvement in selectivity, productivity, and durability without introducing significant additional cost.

The ultimate goal of this study is to analyze effects due to polymerization conditions and imidization methods on properties of 1,3-propanediol monoesterified crosslinkable polyimide (PDMC). Hillock, Omole, Ward, and Ma did work on PDMC synthesis [1-4]; however, variability of polymer properties remains a challenge that must be overcome for industrial implementation of PDMC material.

First, reaction temperature and reaction time of polymerization prior to imidization were considered as key conditions to affect molecular weight, crosslinkability and transport properties of polymer. Batches with controlled reaction temperature and time were prepared, and properties of each dense film were measured and optimized in terms of permeability, selectivity, and plasticization suppression.

Second, imidization methods for PDMC were also studied. There are mainly

two kinds of Imidization: chemical Imidization and thermal Imidization. Surprisingly, thermally imidized PDMC showed 70% higher permeability than chemically imidized samples with minimal sacrifice in selectivity. At high reaction temperature during the thermal imidization, transamidation can occur. It is believed that the transamidation led to more randomized sequence distribution in the thermally imidized samples. We thus hypothesize that the higher permeability of the thermally imidized PDMC results from greater uniformity of the sequence distribution, as compared to the chemically imidized sample that does not experience high temperature during imidization. XRD, DSC, DMA, and permeation instruments checked and supported this hypothesis. FTIR, TGA, and NMR ruled out the possibility of an alternate hypothesis related to side reaction.

Finally, effects of aggressive feed conditions on both chemically imidized PDMC and thermally imidized PDMC dense film were examined. The aggressive feed conditions include high CO_2 partial pressure, operating temperatures, and exposure to high feed pressure. Testing aggressive feed conditions for dense film should be pursued before pursuing hollow fiber applications, to decouple effects on the basic material from those on the more complex asymmetric morphology.

This study enables understanding of the disparity between various previous researchers' selectivity and permeability values. The work shows clearly that polymerization conditions and imidization methods must be specified and controlled to achieve consistently desirable polymer properties. In addition, for batch scale-up and development to a hollow fiber, this fundamental study should enable production of high molecular weight PDMC with good fiber spinnability and defect-free structure.

References

[1] C. Ma, Highly Productive Ester Crosslinkable Composite Hollow Fiber Membranes for Aggressive Natural Gas Separations, Ph.D. Dissertation, in: School of Chemical and Biomolecular Engineering, Georgia Institute of Technology, Atlanta, GA, 2011.

[2] J.K. Ward, CROSSLINKABLE MIXED MATRIX MEMBRANES FOR THE PURIFICATION OF NATURAL GAS, PhD Dissertation, in: School of Chemical & Biomolecular Engineering, Georgia Institute of Technology, Atlanta, GA, 2010.

[3] A.M.W. Hillock, W.J. Koros, Cross-linkable polyimide membrane for natural gas purification and carbon dioxide plasticization reduction, Macromolecules, 40 (2007) 583-587.

[4] I.C. Omole, S.J. Miller, W.J. Koros, Increased molecular weight of a cross-linkable polyimide for spinning plasticization resistant hollow fiber membranes, Macromolecules, 41 (2008) 6367-6375.

CHAPTER 1

INTRODUCTION

1.1 Natural gas overview

Global Natural gas consumption has increased steadily as shown in Figure 1.1 [1]. Estimates suggest annual global natural gas production may reach 153 trillion standard cubic feet by 2030—roughly a 50% increase compared to natural gas production in 2006 [2].

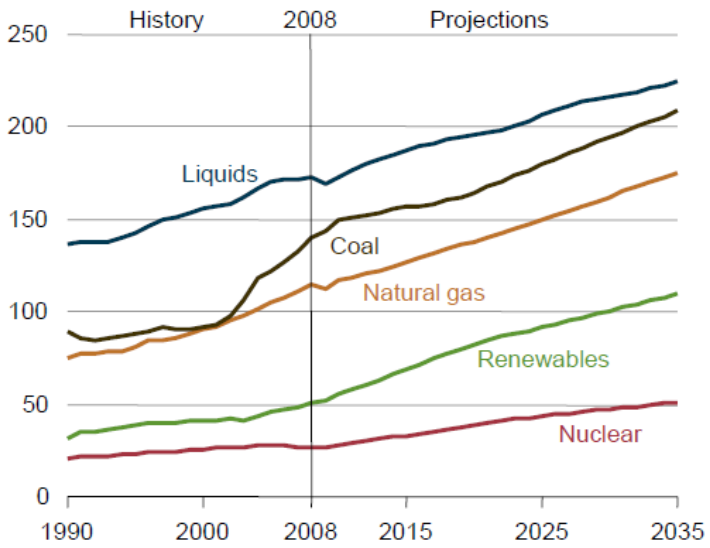

Figure 1.1: World Energy Consumption by fuel [1].

Now, the consumption of natural gas is 22 trillion scf/yr in the U.S. and is 95 trillion scf/yr in the world [2]. In order to meet the predicted amount of natural gas consumption, more improved and efficient membrane technology with minimal processing cost will be necessary.

Compositions of unrefined natural gas vary significantly from source to

source. Usually, a major contaminant of unpurified natural gas is CO_2. The other impurities often include as N_2, H_2S, H_2O, and small hydrocarbons [3]. All the impurities must be reduced to some degree by separation procedure in order to meet U.S. pipeline specifications described in Table 1.1. In some natural gas feeds, CO_2 level can even reach 50%.

Table 1.1 Natural gas pipeline specifications in the U.S. [3].

Component	**Pipeline specifications (U.S.)**
CO_2	< 2%
H_2O	< 120 ppm
H_2S	< 4 ppm
C_{3+} content	950-1050 Btu/scf; Dew point < -20 °C
Inert gases (N_2, He, etc.)	< 4%

1.2 Natural gas separation membranes

In industry, hollow fiber modules are preferred mainly due to the high surface area to volume ratios in the fiber format. Before proceeding to the hollow fiber application and the large-scale production, dense film lab testing is necessary. Using dense films, engineers can measure material transport properties in order to check properties prior to attempting hollow fiber applications. Dense film testing is important in that measured transport properties can be used to calculate selective layer's thickness, and hence the intrinsic material properties. Primarily, this thesis focuses on dense film to set the stage for future hollow fiber work.

Plasticization has been a major problem in polymeric membranes used in aggressive feeds like high-pressure natural gas. Plasticization occurs as testing pressure increases. Along with high testing pressure, permeability increases, and selectivity decreases due to swelling of polymer chains and enhancing chain segmental motions. Introducing ester-based crosslinking has been shown to offer a

remedy for plasticization. Ester-crosslinked polymer (PDMC) shows plasticization suppression up to high enough pressures for most natural gas sources. However, there are still tradeoff limitations between permeability and selectivity even for crosslinked PDMC as shown in Figure 1.2 [4].

Inorganic membrane, carbon molecular sieve, and mixed matrix membrane are intrinsically advantageous over polymeric membrane in terms of performance, and properties can cross above the CO_2/CH_4 upper bound in Figure 1.2. However, polymeric membranes are still more economical in terms of fabrication with adequate separation properties. Moreover, natural gas companies tend to prefer polymeric membranes since the most experience exists for polymeric membranes.

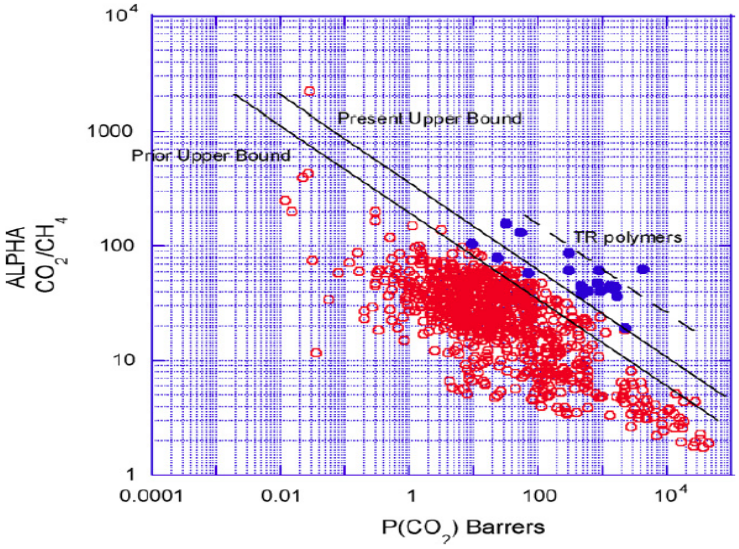

Figure 1.2: Robeson's 2008 upper bound showing the tradeoff between permeability and selectivity for polymer membranes (Prior upper bound: upper bound set in 1991, Present upper bound: upper bound set in 2008, TR polymers: thermally rearranged polymers (mostly considered in the class of molecular sieving materials)) [4].

1.3 Research objectives

(1) Achieve systematic understanding/control of polymerization conditions to develop the optimum chemically imidized PDMC.

PDMC consists of monomers: 6FDA, DAM, and DABA. For PDMC, 6FDA has strong reaction preference for DAM over DABA moiety, and cross-linkages occur through the DABA moiety; therefore, monomer sequence distribution along the polymer backbone may affect polymer properties. We hypothesized that polymerization temperature and reaction time could affect the monomer sequence distribution. For example, monomer sequence could be more randomized through transamidation at higher reaction temperature over sufficient reaction time.

(2) Investigate effects of imidization method on separation performance and polymer properties

There are two types of imidization processes: *Chemical imidization* and *Thermal imidization*. *Chemical imidization* typically occurs at ambient temperature (20℃), while thermal imidization occurs at high temperature (190℃). In the imidization stage, randomization of monomer sequence distribution can occur due to transamidation. Various characterizations and analyses will be reported to explain monomer sequence distribution difference between chemically imidized PDMC and thermally imidized PDMC.

(3) **Demonstrate effects of aggressive feed conditions on both chemically imidized PDMC and thermally imidized PDMC dense film**

In some actual natural gas feeds, feeds are very aggressive. Thus, it is important to characterize effects of the realistic feed conditions on the stability of dense films. The conditions may be detrimental to the separation performance of membranes. Effects of high CO_2 partial pressures and operating temperatures will be

studied with a CO_2/CH_4 mixed gas. Effects of exposure to high-pressure feed will be also studied to simulate realistic feed states.

1.4 Thesis organization

This thesis starts with an explanation of basic concepts, and proceeds to the explanation of detailed discoveries of the study. Chapter 2 introduces essential background knowledge and theory of the topics examined in this research. Chapter 3 describes materials, experimental procedures, and apparatus used in this study. Chapter 4 contains the optimization of polymerization conditions for the performance of chemically imidized PDMC. Chapter 5 discusses the analysis of performance of thermally imidized PDMC. Chapter 6 discusses the effects of aggressive feed on transport properties of chemically imidized PDMC and thermally imidized PDMC. Finally, Chapter 7 provides conclusion of this work, and includes recommendations for future work on this topic.

1.5 References

[1] International Energy Outlook 2010. Report Number: DOE/EIA-0484(2011). Energy Information Administration.

[2] U.S. Energy Information Administration: Independent Statistical Analyses. International Energy Outlook 2009.

http://www.eia.doe.gov/oiaf/ieo/graphic_data_natgas.html.

[3] R.W. Baker, Future directions of membrane gas separation technology. Industrial & Engineering Chemistry Research.

[4] Robeson, L.M., The upper bound revisited. Journal of Membrane Science, 2008. 320: p. 390-400.

CHAPTER 2

BACKGROUND AND THEORY

2.1 Gas transport in polymer membranes

2.1.1 General transport theory

For polymeric membranes investigated in this work, Knudsen diffusion and sorption-diffusion models explain separation performance [1,3]. Knudsen diffusion occurs when the membrane pore size is comparable to or smaller than mean free path of the gas molecules. The diffusivity for Knudsen selectivity is proportional to the inverse square root of the molecular weights of the gas molecules [3]. The calculated selectivity in Knudsen-diffusion is not sufficient for high gas separation performance polymeric membranes. Therefore, the Knudsen diffusion mechanism will not be considered further.

In the sorption-diffusion model, the penetrants first sorb into the upstream side of the membrane and then diffuse through the membrane under a concentration driving force, and finally desorb from the downstream side at a pressure close to zero. Therefore, permeability coefficient (P) of a polymeric membrane can be evaluated by the product of diffusion coefficient (D), and sorption coefficient (S) as shown in Equation 2.1 [1].

$$P = D \cdot S \tag{2.1}$$

As shown in figure 2.1, assuming the selective layer of the polymer membrane is isotropic, the diffusion coefficient (D) can be expressed as a function of the average jumping length (λ) and average jumping frequency, (f), as shown in

Equation 2.2 [1].

$$D = \frac{f \cdot \lambda^2}{6} \tag{2.2}$$

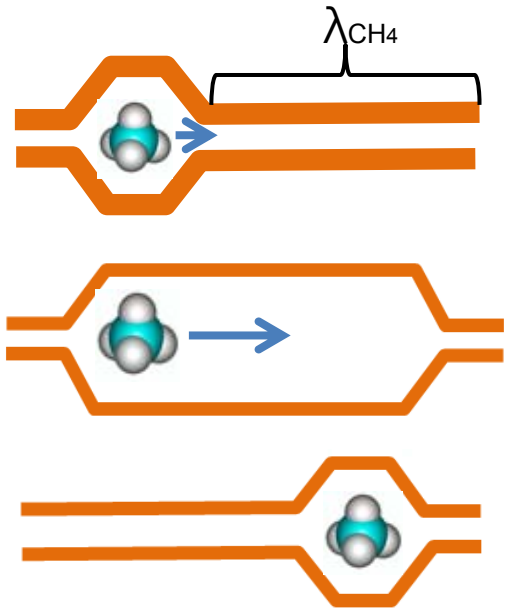

Figure 2.1: Schematics of diffusion through a polymer via transient gap formation. (λ_{CH4}: average jumping length of CH_4)

In a glassy polymer membrane, the sorption coefficient (S_A) is defined as a penetrant's sorption capacity at a given pressure as shown in Equation 2.3 [4].

$$S_A = \frac{C_A}{p_A} = k_{D,A} + \frac{C'_{HA} b_A}{1 + b_A p_A + b_B p_B} \tag{2.3}$$

In Equation 2.3, $k_{D,A}$ is the Henry's law constant; $C'_{H,A}$ and b_A represent the Langmuir capacity constant and Langmuir affinity constant of component A, respectively. p_A is the penetrant pressure of component A.

In the dual-mode sorption model, at low pressure, the Langmuir mode tends to dominate the gas sorption in the membrane, while at high pressure, the microvoids become saturated due to penetrant sorption, and Henry's Law becomes the dominate mode for gas sorption in the membrane.

2.1.2 Characterization of dense film membranes

To evaluate separation performance of a polymeric membrane, permeability and selectivity are commonly used. Permeability is a measure of intrinsic membrane productivity, and it is defined by the flux of penetrant (A), the membrane thickness (l) and the partial pressure or fugacity difference across the membrane (Δp_A), as shown in Equation 2.4 [1].

$$P_A = \frac{N_A \times l}{\Delta p_A} \tag{2.4}$$

In Equation 2.4, N_A represents the flux of penetrant A across the membrane; l refers the membrane thickness; Δp_A represents the partial pressure or fugacity difference of penetrant A across the membrane. The common unit of permeability is the Barrer, as shown in Equation 2.5.

$$\text{Barrer} = 10^{-10}\left(\frac{cc(STP)}{cm^2 \cdot s}\right) \cdot \frac{cm}{cmHg} \tag{2.5}$$

Selectivity is a measure of intrinsic membrane efficiency, and is equal to the ratio of the two gas permeability when the downstream pressure is negligible compared to the upstream pressure. Ideal selectivity is shown in Equation 2.6.

$$\alpha_{AB} = \frac{P_A}{P_B} \tag{2.6}$$

For mixed gas permeation, complications including swelling effects, non-infinite feed to permeate pressure ratio, sorption site competition and so-called "frame of reference" effects could occur [5]. In general, the separation factor, $(S.F.)_{AB}$, is written as

$$(S.F.)_{AB} = \frac{y_A/y_B}{x_A/x_B} \quad (2.7)$$

In equation 2.7, x refers to the mole fraction of the gas component in the downstream, and y refers to the mole fraction of the gas component in the upstream feed to the membrane [6].

2.1.3 Plasticization of polymer membranes

Plasticization occurs in glassy polymers when a sorbed penetrant swells the polymer matrix and increases segmental mobility, thereby increasing free volume. The increase in free volume results in loss in the shape discrimination and leads to increased diffusion coefficients of each penetrant, thereby increasing the permeability. For CO_2/CH_4 separation, plasticization impact on slower component CH_4 is greater because increased free volume could provide CH_4 molecules with higher diffusivity increase. As a result, in the presence of plasticization, decrease of selectivity occurs with an increase in permeability. As shown in Table 2.1, carbon dioxide, whose critical temperature is relatively high, interacts with glassy polymers strongly and has high solubility in polar polymers. Since natural gas contains non-negligible carbon dioxide, plasticization phenomenon could be a problem in natural gas purification.

Table 2.1: Kinetic diameters and critical temperatures for practical gases [7].

	Helium	Carbon dioxide	Oxygen	Nitrogen	Methane
Kinetic Diameter (Å)	2.60	3.30	3.46	3.64	3.80
Critical Temperature (K)	5.2	304.2	154.4	126.1	190.7

The plasticization pressure defines the point where permeability begins to increase as shown in Figure 2.2 [8]. Below the plasticization pressure, permeability asymptotically decreases as penetrant pressure increases, due to saturation of Langmuir sorption sites. However, above the plasticization pressure, permeability increases significantly, as sorption of Henry's mode and swelling of polymer chains starts.

Covalently crosslinkable polyimide offers a good option for stabilization against plasticization [9]. Once polymer chains form a network matrix, the polymer matrix shows enhanced plasticization resistance at higher feed pressures of highly-swelling penetrants.

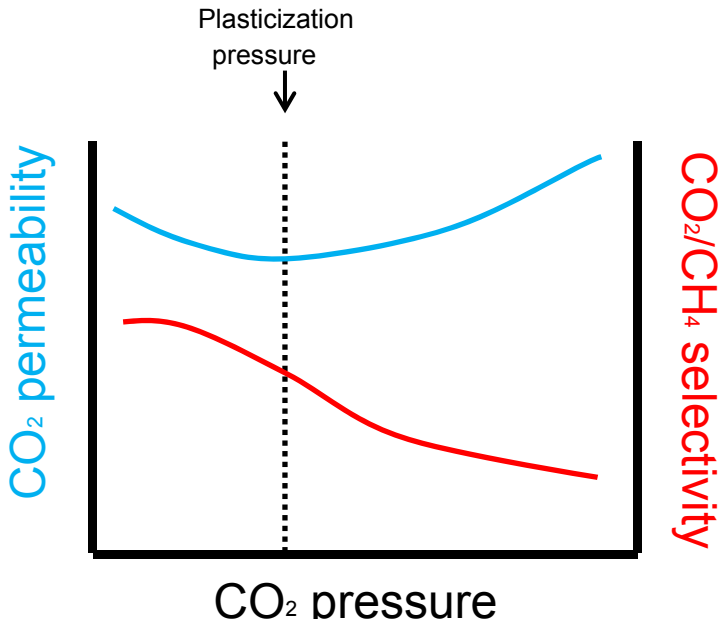

Figure 2.2: Schematics of permeability increase and selectivity decrease due to membrane plasticization.

Covalently crosslinkable polyimides can contain diaminobenzoic acid (DABA) groups which act as sites for crosslinking between polymer chains. Previous researchers studied diol-crosslinking agents such as ethylene glycol, 1,3-prodanediol,

propylene glycol, 1,4-butanediol, and 1,4-cyclohexanedimethanol. 1,3-propanediol showed adequate reactivity and minimal effects on the separation properties of the dense film. Hillock and Wind also showed that crosslinked PDMC exhibits plasticization suppression at high pressure in dense films [10-14].

2.1.4 Physical aging

The amounts of excess free volume in glassy polymers depend on synthesis conditions, thermal history, and previous gas exposure. As shown in Figure 2.3, the elimination of excess free volume or unrelaxed volume due to relaxation of polymer chain to equilibrium conformations is termed physical aging [15-20]. The physical aging can result in time dependence of membrane transport properties. As physical aging occurs, permeability tends to decrease and selectivity tends to increase. Due to a diffusion-like mechanism, physical aging accelerates with increasing temperature and decreasing membrane thickness.

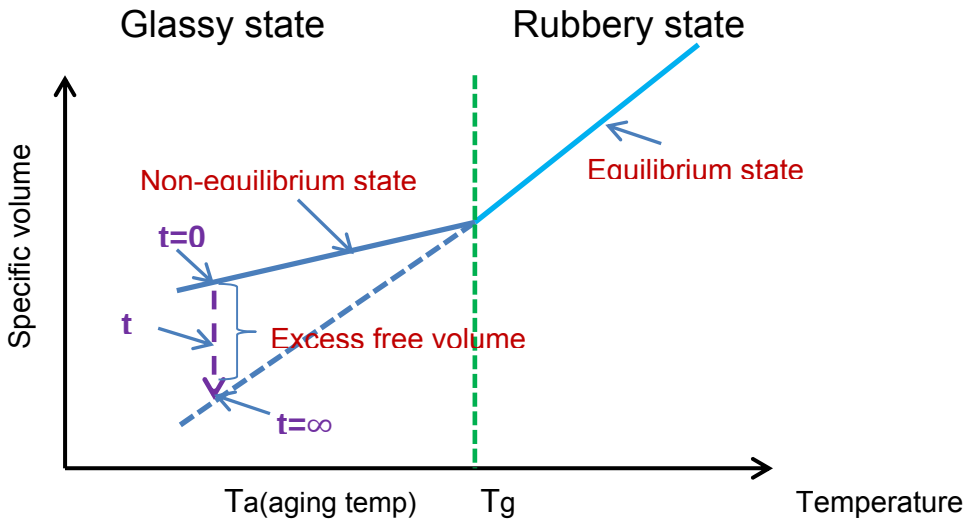

Figure 2.3: Schematic illustration of the specific volume vs. T for a glassy polymer.

2.2 Copolymer and transamidation

Copolymers are derived from repeating sequences of two monomeric species. As shown in Figure 2.4, there are mainly two kinds of copolymer: random copolymer, and block copolymer. If the probability of finding a specific monomer in the sequence is equal to the mole fraction of that monomer residue in the chain, then the polymer is a random copolymer. Block copolymer comprises two homopolymer subunits linked by covalent bonds.

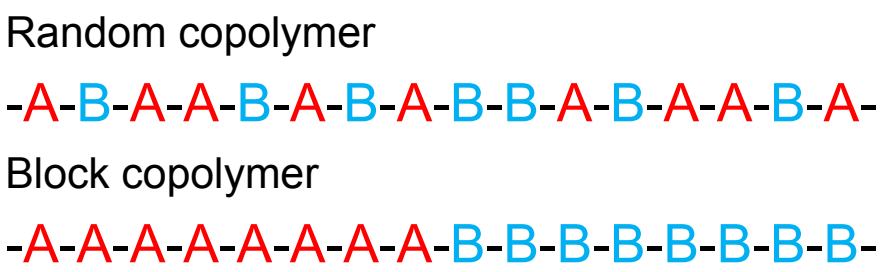

Figure 2.4: Schematic illustration of random copolymer and block copolymer including A and B, where A is 6FDA-DAM and B is 6FDA-DABA in this work.

Polyimides used in this work consist of two monomer units: 6FDA-DAM (A) and 6FDA-DABA (B). Dianhydride 6FDA could react with diamines DAM and DABA, but DAM and DABA could not react with each other. If the monomer 6FDA prefers DAM to DABA significantly, monomers 6FDA and DAM will form covalent bonds first, and then the rest of 6FDA starts to react with DABA as shown in block copolymer. DAM actually has higher reactivity than DABA due to three electron donating methyl groups that makes DAM a better nucleophile.

As will be seen in the chapter 3, transamidation during thermal imidization is possible at high temperature (190℃). Transamidation is defined as the transferal of an amide group from one compound to another. Generally, there are three kinds of

transamidation: aminolysis, acidolysis, and amidolysis. Transamidation is potentially a synthetically useful reaction, but is hindered by high stability of the carboxamide group. Several reports showed that thermal transamidation reactions typically require very high temperature over 180 ℃ [21]. The transferal converts a block copolymer to a random copolymer as described in Figure 2.5. Specifically, order of 6FDA-DAM (A) and 6FDA-DABA (B) becomes more random as transamidation takes place during thermal imidization because of high temperature.

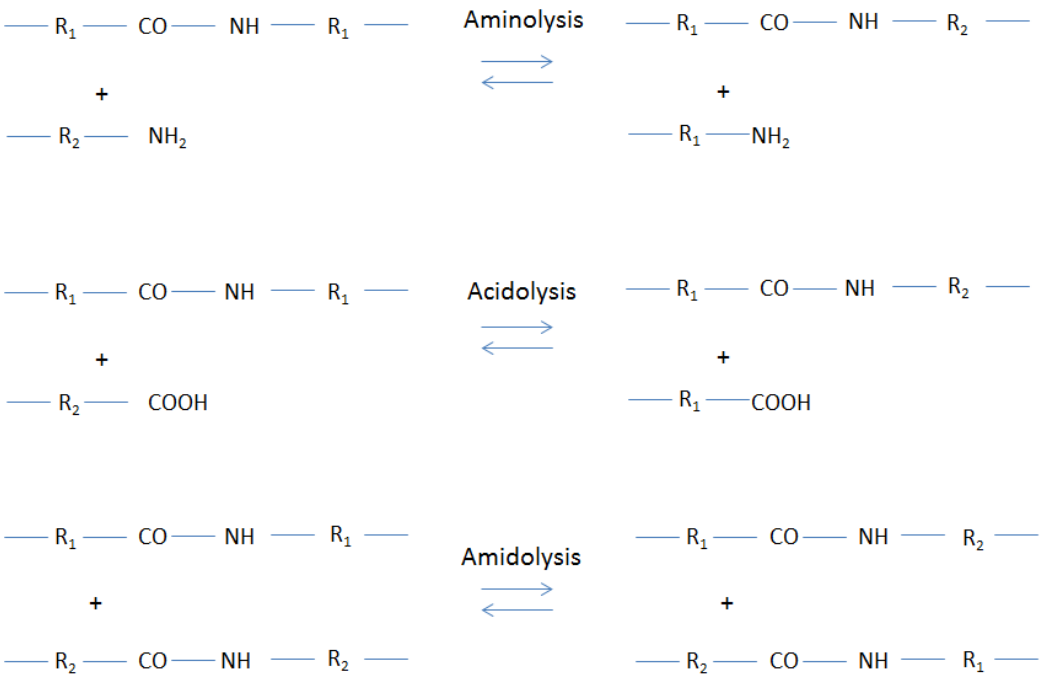

Figure 2.5: Three kinds of transamidation: aminolysis, acidolysis, and amidolysis [22].

2.3 References

[1] W.J. Koros, G.K. Fleming, Membrane-Based Gas Separation, J Membrane Sci, 83 (1993) 1-80.

[2] M. Mulder, Basic principles of membrane technology, 2nd ed., Kluwer Academic, Dordrecht ; Boston, 1996.

[3] R.W. Baker, Membrane technology and applications, 2nd ed., J. Wiley, Chichester ; New York, 2004.

[4] W.J. Koros, R.T. Chern, V. Stannett, H.B. Hopfenberg, A Model for Permeation of Mixed Gases and Vapors in Glassy-Polymers, J Polym Sci Pol Phys, 19 (1981) 1513-1530.

[5] H. Denny Kamaruddin, W.J. Koros, Some Observations about the Application of Fick's First law for Membrane Separation of Multicomponent Mixtures, J. Membr. Sci. 135 (1997) 147–159.

[6] I.C. Omole, R.T. Adams, S.J. Miller, W.J. Koros, Effects of CO2 on a High Performance Hollow-Fiber Membrane for Natural Gas Purification, Ind Eng Chem Res, 49 (2010) 4887-4896.

[7] Ho, W.S.W. and K.K. Sirkar, eds. Membrane Handbook. 1992, Van Nostrand Reinhold: New York, NY.

[8]]I.C. Omole, Crosslinked Polyimide Hollow Fiber Membranes for Aggressive Natural Gas Feed Streams, Ph.D. Dissertation, in: Chemical and Biomolecular Engineering, Georgia Institute of Technology, Atlanta, GA, 2008.

[9] J.D. Wind, C. Staudt-Bickel, D.R. Paul, W.J. Koros, Solid-state covalent crosslinking of polyimide membranes for carbon dioxide plasticization reduction, Macromolecules 36 (2003) 1882–1888.

[10] J.D. Wind, S.M. Sirard, D.R. Paul, P.F. Green, K.P. Johnston, W.J. Koros,

Carbon dioxide-induced plasticization of polyimide membranes: Pseudo-equilibrium relationships of diffusion, sorption, and swelling, Macromolecules, 36 (2003) 6433-6441. 30

[11] J.D. Wind, C. Staudt-Bickel, D.R. Paul, W.J. Koros, The effects of crosslinking chemistry on CO_2 plasticization of polyimide gas separation membranes, Ind Eng Chem Res, 41 (2002) 6139-6148.

[12] A.M.W. Hillock, W.J. Koros, Cross-linkable polyimide membrane for natural gas purification and carbon dioxide plasticization reduction, Macromolecules, 40 (2007) 583-587.

[13] A.M.W. Hillock, S.J. Miller, W.J. Koros, Crosslinked mixed matrix membranes for the purification of natural gas: Effects of sieve surface modification, J Membrane Sci, 314 (2008) 193-199.

[14] J.D. Wind, Improving Polyimide Membrane Resistance to Carbon Dioxide Plasticization in Natural Gas Separations, PhD dissertation, in: Chemical Engineering, The University of Texas at Austin, Austin, TX, 2002.

[15] Adam, K., Thickness Dependent Physical Aging and Supercritical Carbon dioxide Conditioning Effects on Crosslinkable Polyimide Membranes for Natural Gas Purification, in Chemical & Biomolecular Engineering. 2008, Georgia Institute of Technology: Atlanta. p. 200.

[16] Kim, J.H., W.J. Koros, and D.R. Paul, Effects of CO_2 exposure and physical aging on the gas permeability of thin 6FDA-based polyimide membranes: Part 2. with crosslinking. J. Membr. Sci., 2006. **282**(1-2): p. 32-43.

[17] Kim, J.H., W.J. Koros, and D.R. Paul, Physical aging of thin 6FDA-based polyimide membranes containing carboxyl acid groups. Part I. Transport properties. Polymer, 2006. **47**(9): p. 3094-3103.

[18] Kim, J.H., W.J. Koros, and D.R. Paul, Physical aging of thin 6FDA-based

polyimide membranes containing carboxyl acid groups. Part II. Optical properties. Polymer, 2006. **47**(9): p. 3104-3111.

[19] Moe, M.B., W.J. Koros, and D.R. Paul, Effects of molecular structure and thermal annealing on gas transport in two tetramethylbisphenol A polymers. J. Polym. Sci., Part B: Polym. Phys., 1988. **26**(9): p. 1931-45. 52.

[20] Jordan, S.M., W.J. Koros, and G.K. Fleming, The effects of carbon dioxide exposure on pure and mixed gas permeation behavior: comparison of glassy polycarbonate and silicone rubber. J. Membr. Sci., 1987. **30**(2): p. 191-212.

[21] C. L. Allen, B. N. Atkinson and J. M. J. Williams, Transamidation of Primary Amides with Amines Using Hydroxylamine Hydrochloride as an Inorganic Catalyst. Angew. Chem., 1383. Int. Ed., 2012, 51,

[22] A.M. Kotliar, J., Interchange reactions involving condensation polymers, Polym. Sci., Macromol. Rev., 16, 367 (1981)

CHAPTER 3

MATERIALS AND PROCEDURES

3.1 Materials

3.1.1 Polyamic acid synthesis

The polyamic acid was synthesized via a polycondensation reaction between (4,4'hexafluoroisopropylidene) diphthalic anhydride (6FDA) (99%, Lancaster Synthesis, WardHill, MA), 2,4,6-trimethyl-m-phenylenediamine (DAM) (96%, Sigma-Aldrich, St. Louis, MO), and 3,5-diaminobenzoic acid (DABA) (98%, Sigma-Aldrich) in 1-methyl-2-pyrrolidinone (NMP) (anhydrous, 99.5%, Sigma-Aldrich). Monomer ratio between DAM and DABA is 3:2. The monomer ratio is chosen because of high CO_2/CH_4 separation performance and high CO_2-induced plasticization suppression shown in previous work [1-3]. The reaction scheme is displayed in Figure 3.1.

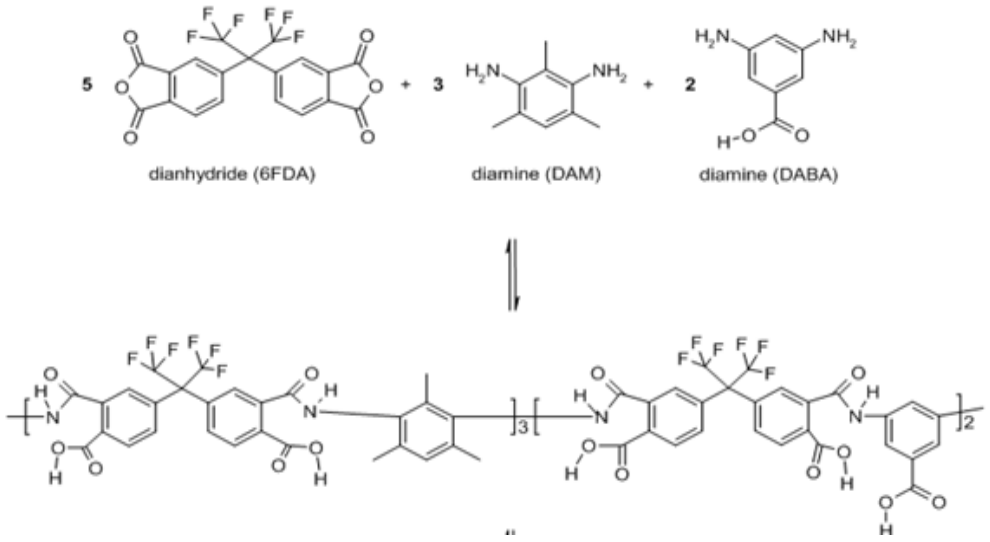

Figure 3.1: Reaction scheme for polycondensation reaction from monomer to 6FDA-DAM: DABA (3:2) polyamic acid.

3.1.2 Imidization

Imidization processes close imide rings in polymeric acid precursor chains. There are two kinds of imidization: chemical imidization and thermal imidization. Chemical imidization typically uses imidization catalyst (beta picoline) and a dehydrating agent (acetic anhydride) at low temperature below 20℃. Because of the low imidization temperature, the chemical imidization is advantageous for avoiding undesirable thermally activated side reactions, but it is prone to form isoimides [3].However, polymer precipitated by methanol is subsequently thermally treated at 210℃ to convert isoimides to imides, complete imidization, and prevent chain scissoning during the following monoesterification [4-6].The precipitated polymer needs to be dissolved again in NMP for subsequent monoesterification to react 1,3-propanediol with imidized 6FDA-DAM-DABA (3:2), which makes this approach a “two-pot” method.

On the contrary, thermal imidization occurs by simply heating the polymer solution to a high temperature about 190℃. For removing by-product water produced from imidization, ortho-dichlorobenzene (ODCB) is used as a dehydrating agent. Following thermal imidization, monoesterification occurs without polymer precipitation since heat treatment of polymer is not required, which makes this approach a “one-pot” method [3]. These references describe details of synthesis. The reaction scheme is displayed in Figure 3.2.

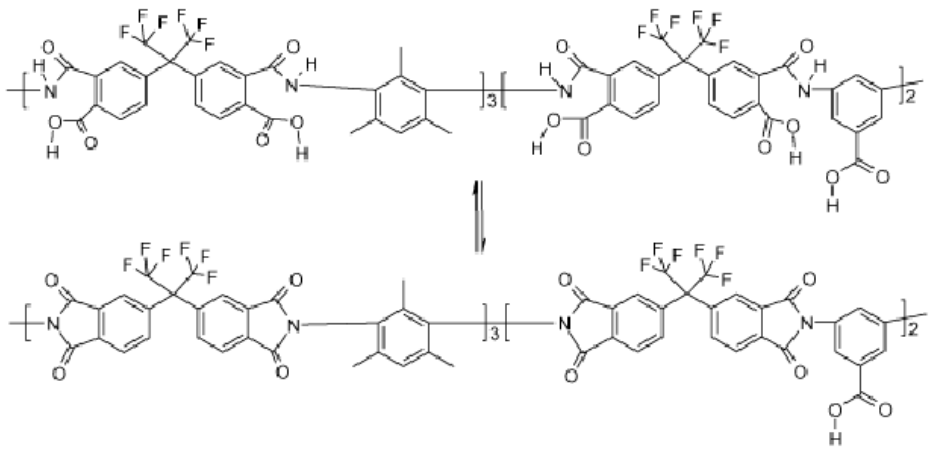

Figure 3.2: Reaction scheme for imidization from polyamic acid to 6FDA-DAM:DABA (3:2) polyimide.

During a thermal imidization, it is believed that transamidation can occur. At high reaction temperature during the thermal imidization, transamidation occurs. It is believed that the transamidation leads to more randomized sequence distribution in the thermally imidized samples [7]. This hypothesis was covered in section 2.2.

3.1.3 Monoesterification

Various alcohols such as 1,3-propanediol, ethylene glycol, butylene glycol 1,4-benzenedimethanol, and 1,4-cyclohexanedimethanol can react with carboxylic acid groups in DABA moiety of imidized 6FDA-DAM-DABA (3:2) to make covalent ester bonds. Especially, 1,3-propanediol shows desirable transport properties when the alcohol formed ester bonds with imidized 6FDA-DAM-DABA (3:2) [8]. The imidized polymer was esterified using 1,3-propanediol (99.6%, Sigma-Aldrich) and p-toluenesulfonic acid (p-TSA) (98.5%, Sigma-Aldrich) as a catalyst. Byproduct water coming off from monoesterification can cause hydrolytic attack of imide rings and result in significant loss of molecular weight. Molecular weight loss was prevented by

both reducing the amount of catalyst by half and lowering the reaction temperature from 140℃ to 130℃ The reaction scheme for the monoesterification is demonstrated in Figure 3.3. Details of synthesis procedure can be found in the Appendix C.

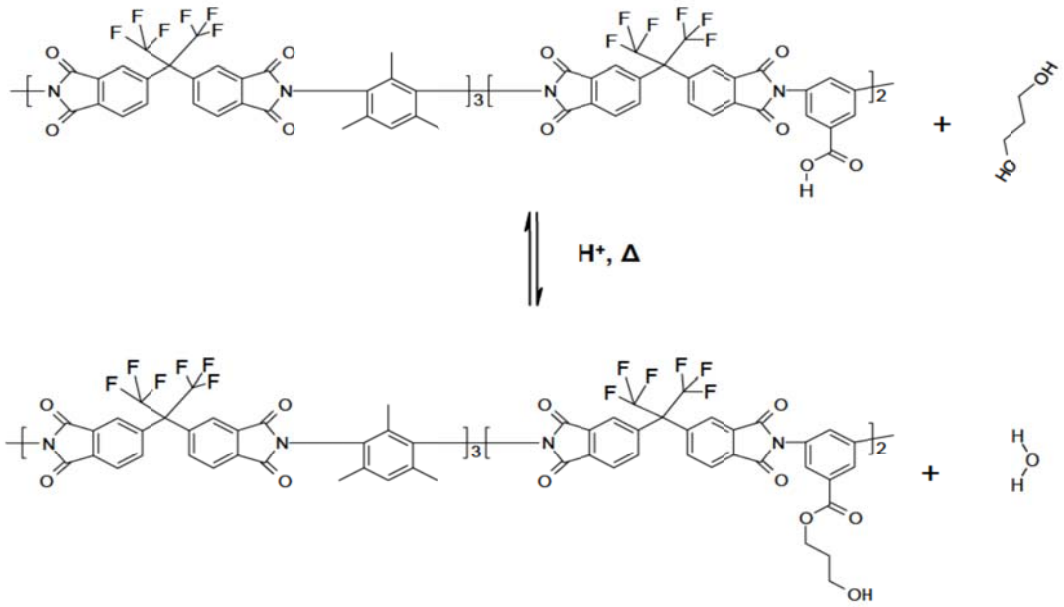

Figure 3.3: Reaction scheme for monoesterification of 6FDA-DAM:DABA (3:2) with 1,3-propanediol to form PDMC.

3.2 Dense film membrane preparation

PDMC polymer films were formed by a solution casting method [9]. Tetrahydrofuran (THF) and polymer was mixed to make a solution. The 3 wt% solution was cast onto Teflon dishes in the glove bag fully saturated by THF. After 3 days, the film was removed and dried at 70°C overnight to remove any residual THF. After the oven was preheated up to 200°C, the film was put in the oven for 2 hours. The film was cooled down to room temperature in the oven after the treatment.

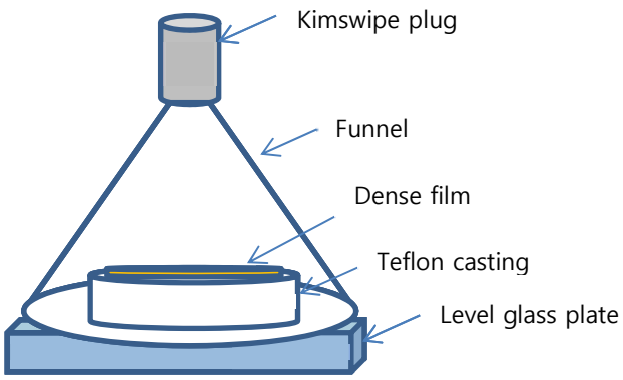

3.3 Dense film characterization techniques

3.3.1 Pure gas permeation

Films were mounted onto the permeation cell, and CO_2/CH_4 selectivity was measured at 65 psi, 35°C using pure gases. In order to show plasticization suppression over high CO_2 pressure, all of the PDMC films were subsequently tested up to 500 psi. For pure gas permeation, mixed gas venting in the upstream and GC analysis is not necessary.

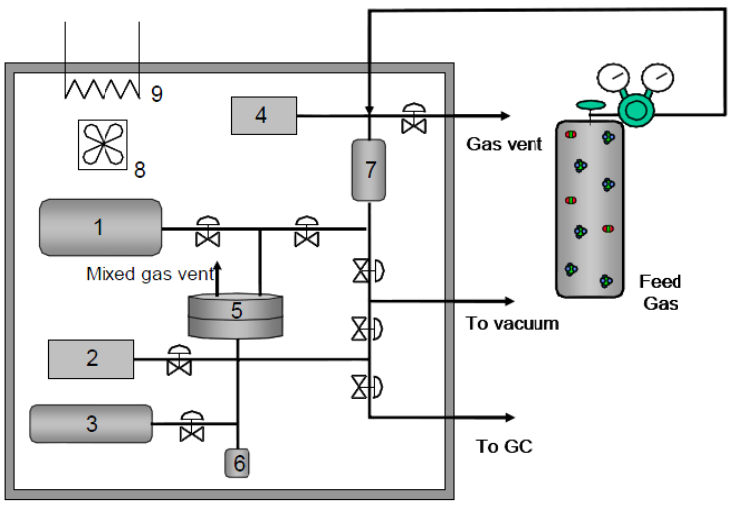

Equation 3.1 [3] determines the permeability of a dense film membrane.

$$\mathrm{P} = \frac{1.1583\times 1o^{3}\times(\frac{dp}{dt})\times l\times V_R}{A\times T\times \Delta p} \qquad (3.1)$$

In Equation 3.1, dp/dt is the slope of the downstream pressure versus time (torr/min); l (μm) is the thickness of membrane; V_R (cm^3) is the volume of downstream reservoir; A (cm^2) is the area of dense film; T (K) is the operating temperature. p represents the partial pressure or fugacity difference acting between the upstream and downstream face of the membrane.

3.3.2 Mixed gas permeation

Films were also mounted onto the permeation cell. CO_2/CH_4 selectivity was measured at 65 psi, 35°C using mixed gas. In order to show plasticization suppression over high CO_2 pressure, all of the PDMC films were tested up to 800 psi. Mixed gas permeation requires a mixed gas venting in the upstream and connection to GC devices. The permeation system is depicted in Figure 3.5 in section 3.3.1. For mixed gas permeation, it is important to control stage cut (permeate flow / feed flow) below 1% by venting the upstream to avoid concentration change at the upstream of the dense film. Agilent Technologies 6890N Network GC system and ChemStations software determined the gas flow compositions. Ultra high purity level helium was used as the carrier gas. Details of the mixed gas permeation system can be found in reference [3].

3.3.3 Gel Permeation Chromatography (GPC)

GPC was conducted to analyze the molecular weight and polydispersity index of the samples synthesized in this study. Mono-disperse polymer standards (solution of 15 mg mono-dispersed polystyrene in 2ml THF) were adopted to plot the logarithm of the molecular weight versus the retention volumes or retention times. The solution was filtered by 0.45 um size filter. Measurement in this work uses RI detector.

3.3.4 Fourier-Transform Infrared spectroscopy (FTIR)

The FTIR in this work was done using a Bruker Tensor 27 FTIR spectrometer. FTIR offers information about the functional groups of sample. Polymer film samples were analyzed using a Harrick MVP_2 micro ATR with 128 scans at a resolution of $2cm^{-1}$.

3.3.5 Thermo Gravimetric Analysis (TGA)

Thermo Gravimetric Analysis (TGA) was conducted on a thermogravimetric analyzer (Q5000, TA Instruments) at a heating rate of 10 K/min under nitrogen atmosphere.

3.3.6 X-ray diffraction crystallography (XRD)

The diffraction pattern of copper metal was measured with X-ray radiation. The wavelength of XRD was 1.54 Å. X-ray diffraction crystallography (XRD) was conducted to measure the average spacing between layers or rows of atoms.

3.3.7 Differential Scanning Calorimetry (DSC)

The glass transition temperatures (T_g) of polymers were determined using a differential scanning calorimeter (Q200, TA Instruments). The measurement was carried out using a standard heating-cooling-heating procedure at heating/cooling rates of 10 K/min in nitrogen atmosphere. The sample was heated to beyond its expected glass transition temperature but below its decomposition temperature determined from TGA. The glass transition temperature was determined as the inflection point of the change in the heat flow during the second heating cycle.

3.3.8 Dynamic Mechanical Analysis (DMA)

The modulus of polymers as a function of temperature was analyzed using a dynamic mechanical analysis (Q800, TA Instruments). Dense films were analyzed at heating rates of 3K/min under 0.06% strain at 1 Hz without nitrogen purge.

3.3.9 Nuclear magnetic resonance spectroscopy (NMR)

^{1}H NMR experiments were conducted in solution. The solution NMR studies were performed by dissolving samples in deuterated Dimethyl sulfoxide (DMSO) at 2~2.5 wt%. The solutions were analyzed using a Varian Mercury VX-300 spectrometer to quantify polyimide peaks. ^{13}C NMR experiments were done in solid state using a Bruker DSX 300 with the following specifications: 7 mm MAS rotor, 300 MHz 1H, pulse sequence: CP-MAS with TOSS to suppress spinning side bands, spinning speed: 5 kHz, repetition delay of 4 s, contact time of 1 ms, 90 degree pulse length: 5 microseconds, number of scans: 10K.

3.3.10 Gel fraction test

Cross-linked membranes were immersed in THF solvent at room temperature for two days in order to measure the gel fraction inside. After two days, insoluble fraction was taken out of THF solvent and dried at 100°C in a vacuum oven for a day to evaporate residual solvent from membranes. The gel fractions were calculated by W_i/W_o, where W_i and W_o were the insoluble fraction's weight and original cross-linked membrane's weight respectively.

3.4 References

[1] A.M.W. Hillock, W.J. Koros, Cross-linkable polyimide membrane for natural gas purification and carbon dioxide plasticization reduction, Macromolecules, 40 (2007) 583-587.

[2] D.W. Wallace, C. Staudt-Bickel, W.J. Koros, Efficient development of effective hollow fiber membranes for gas separations from novel polymers, J Membrane Sci, 278 (2006) 92-104.

[3] I.C. Omole, Crosslinked Polyimide Hollow Fiber Membranes for Aggressive Natural Gas Feed Streams, Ph.D. Dissertation, in: Chemical and Biomolecular Engineering, Georgia Institute of Technology, Atlanta, GA, 2008.

[4] M.H. Kailani, C.S. Sung, S.J. Huang, Syntheses and Characterization of Model Imide Compounds and Chemical Imidization Study, Macromolecules, 25 (1992) 3751-3757.

[5] M.H. Kailani, C.S.P. Sung, Chemical imidization study by spectroscopic techniques. 2. Polyamic acids, Macromolecules, 31 (1998) 5779-5784.

[6] M.H. Kailani, C.S.P. Sung, Chemical imidization study by spectroscopic techniques. 1. Model amic acids, Macromolecules, 31 (1998) 5771-5778.

[7] C. L. Allen, B. N. Atkinson and J. M. J. Williams, Transamidation of Primary Amides with Amines Using Hydroxylamine Hydrochloride as an Inorganic Catalyst. Angew. Chem., 1383. Int. Ed., 2012, 51,

[8] J.D. Wind, Improving Polyimide Membrane Resistance to Carbon Dioxide Plasticization in Natural Gas Separations, PhD dissertation, in: Chemical Engineering, The University of Texas at Austin, Austin, TX, 2002.

[9] Adam, K., Thickness Dependent Physical Aging and Supercritical Carbon dioxide Conditioning Effects on Crosslinkable Polyimide Membranes for Natural Gas Purification, in Chemical & Biomolecular Engineering. 2008, Georgia Institute of Technology: Atlanta. p. 200.

CHAPTER 4

OPTIMIZATION OF POLYMERIZATION CONDITIONS FOR THE PERFORMANCE OF CHEMICALLY IMIDIZED PDMC

4.1 Introduction

To explore variability of polymer samples, polymer properties and transport properties as a function of polymerization temperature and reaction time prior to imidization are explored in Chapter 4. This chapter discusses the details of optimization of polymerization conditions for the best performance of *chemically imidized* polyimide PDMC. In this work, polymer properties and transport properties depend on three factors: molecular weight, randomization extent, and side reactions.

First, after sufficient polymerization time, high molecular weight polymer can be synthesized due to higher conversion of monomers. However, unnecessarily long polymerization times should be avoided because of added manufacturing costs for the producer. Polymerization itself is exothermic, and therefore from thermodynamics, the equilibrium conversion decreases as the temperature increases. However, at temperatures (0℃~20℃) examined in this study, it was observed that higher polymerization temperatures resulted in higher conversions. This can be explained by the hypothesis that equilibrium conversion of monomers is not obtained. As polymerization temperature increases, the reaction rate constant increases and the final conversion increases. After all, increased reaction rate constant seems to have more significant impact on conversion than equilibrium shift toward monomers because equilibrium conversion is not obtained yet. This hypothesis is also in good agreement with literature [1,2]. Nevertheless, we wanted to verify that molecular weight builds as temperature increases at temperatures (0℃~20℃) examined in this study, and we found this to be true by experiments. In addition, the fact that

molecular weight keeps rising up until 72 hours in this work supports the expectation that kinetics is an influential factor during the polymerization. However, at mid-range temperatures (20℃~50℃), an equilibrium shift toward monomers seems to be more significant than increase of rate constant as polymerization temperature increases. As a result, as polymerization time increases, molecular weight decreases. Therefore, in order to avoid low molecular weight polymer, all the polymers in this work were polymerized at low temperatures (0℃~20℃). Generally, high molecular weight PDMC shows low permeability and high selectivity due to less chain ends.

Second, as polymerization time increases, monomer sequence distribution can be more randomized. As monomers distributed along polymer chains randomize, the polymer may show changes in transport, due to more randomly dispersed highly permeable DAM monomers. This may make the polymer more permeable and less selective than a case in which low permeability and high permeability blocks exist; however, the precise outcome is difficult to predict. In addition, as polymerization temperature increases, more rapid randomization is expected to occur, since any initially non-random distribution would be expected to randomize more quickly due to more rapid kinetics.

Third, at high polymerization temperature, side reactions such as isoimide formation can lower the yield of polyimide, which possibly contributes to loss of selectivity. To clarify the side reaction's existence, ^{1}H NMR would be necessary.

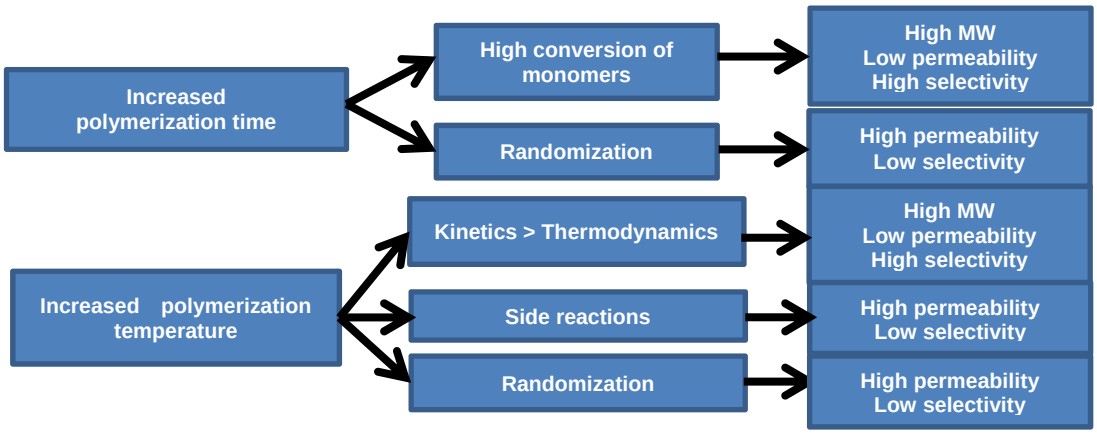

Figure 4.1: Flowchart of possible optimization of *chemically imidized* PDMC related to different potentially controlling factors.

4.2 Effect of polymerization conditions on molecular weight of *chemically imidized* PDMC

Table 4.1: Polymerization conditions. The italic numbers refer to state number identifiers.

t \ T	0 ℃	5 ℃	20 ℃	t \ T	0 ℃ → 20 ℃
6 hr			*7*	3 hr → 21 hr	*11*
24 hr	*1*	*4*	*8*		
48 hr	*2*	*5*	*9*		
72 hr	*3*	*6*	*10*		

To optimize polymerization conditions (shown in Table 4.1), temperature (0 ℃, 5 ℃, and 20 ℃) and time (6 hr, 24 hr, 48 hr, and 72 hr) were chosen as independent variables.

Previous researchers have focused on an alternate state 11 in which 0℃ is used for 3 hours followed by 20℃ for 21 hours, and they reported that a state 11

produced high quality final polyimide [3]. Thus, we tested the state 11 additionally since one may prefer to avoid the need for unnecessarily extended polymerization time. Basically, the idea here is that during the first 3 to 6 hours at 0 ℃, equilibrium of exothermic polymerization can favor the formation of polyamic acid, and for the next 18 to 21 hours at 20 ℃, building of molecular weights occur subsequently due to high reactivity and mobility of polymer chains at the higher temperature.

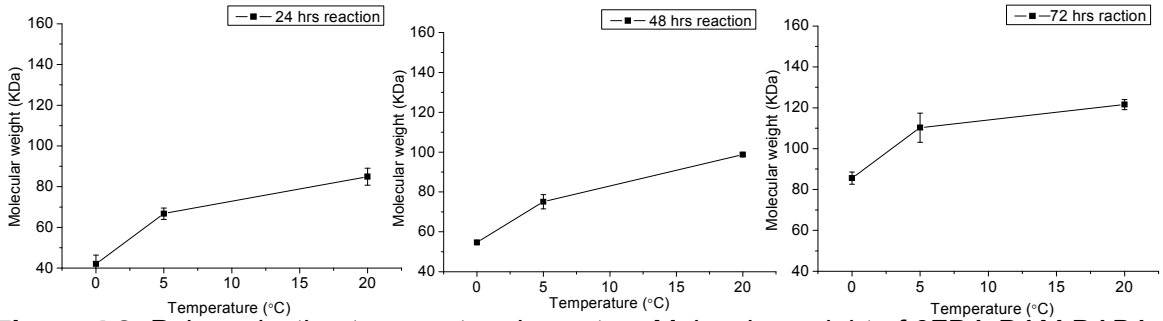

Figure 4.2: Polymerization temperature impact on Molecular weight of 6FDA-DAM:DABA (3:2)

As shown in Figure 4.2, the molecular weight of 6FDA-DAM:DABA (3:2) increases as polymerization temperature increases. State 9 shows the highest molecular weight among states 2, 5, and 9. In a similar way, state 10 shows the highest molecular weight among states 3, 6, and 10. This trend could be explained by *kinetics' dominance over thermodynamics*. Specifically, although the reaction is exothermic and thermodynamics suggest a more favorable equilibrium conversion at lower temperature, the opposite is observed because kinetics is a dominant factor at play in the current set of states. According to the flow chart in Figure 4.1, increased polymerization temperature tends to make high molecular weight PDMC.

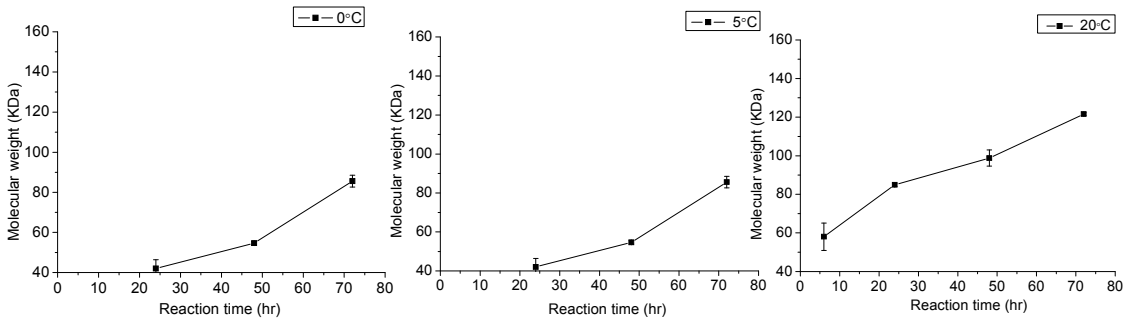

Figure 4.3: Polymerization time impact on Molecular weight of 6FDA-DAM:DABA (3:2).

As shown in Figure 4.3, for the states whose reaction temperatures are the same, as reaction time increases, molecular weight increases due to higher conversion of monomers. After 72 hours of polymerization at 5℃ and 20℃, the PDMC molecular weight reached molecular weight above 140K, which is high enough to spin fibers in the future work.

4.3 Effect of polymerization conditions on transport properties of *chemically imidized* PDMC

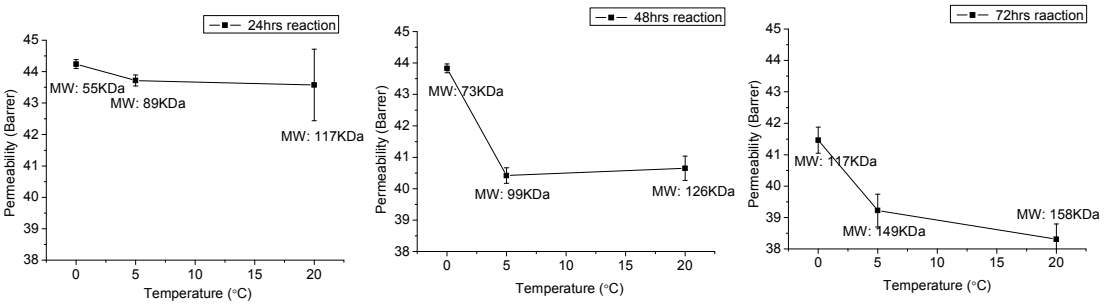

Figure 4.4: Polymerization temperature impact on CO_2 permeability.

As shown in Figure 4.4, given the same polymerization time, PDMC polymerized at low temperature (0℃) shows the highest permeability. At low polymerization temperature, the molecular weight of PDMC tends to be low because

of low conversion of monomers. Low molecular weight PDMC generally contains additional number of chain ends with higher free volume than standard segments, which makes such polymers more permeable. Considering only the molecular weight effect first, as polymerization temperature increases, the permeability of PDMC decreases due to higher molecular weight [4]. Surprisingly, however, PDMC polymerized at 20℃ shows permeability similar to PDMC polymerized at 5℃ for 24hour reaction time and 48hour reaction time. At room temperature (20℃), the anticipated randomization effect can be more significant or side reactions which make polymer permeable could occur. Thus, at room temperature, the randomization extent or side reactions can cloud the molecular weight effect, These issues will be verified by XRD in section 5.8.

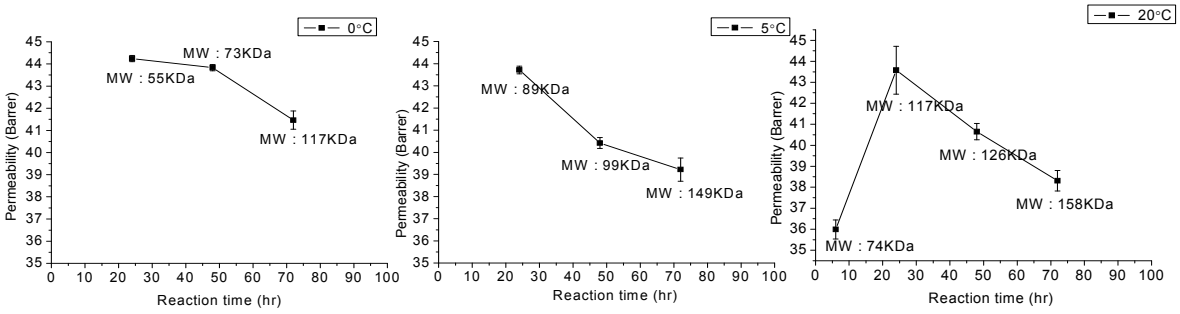

Figure 4.5: Polymerization time impact on CO_2 permeability.

As shown in Figure 4.5, given the same polymerization temperature, as reaction time increases, permeability decreases. As reaction time increases, the molecular weight of PDMC increases due to higher conversion of monomers. Higher molecular weight makes PDMC films less permeable. Thus, considering only molecular weight effects, as reaction time increases, permeability should decrease, which exactly describes Figure 4.5. In this case, the molecular weight effect is dominant over randomization effect. At the same polymerization temperature, randomization effect and side reactions effect by extended polymerization time

seems minimal compared to molecular weight effect, which is verified by XRD in section 5.8. PDMC synthesized for only 6 hours at 20℃ shows particularly low permeability possibly due to blockiness from short polymerization time.

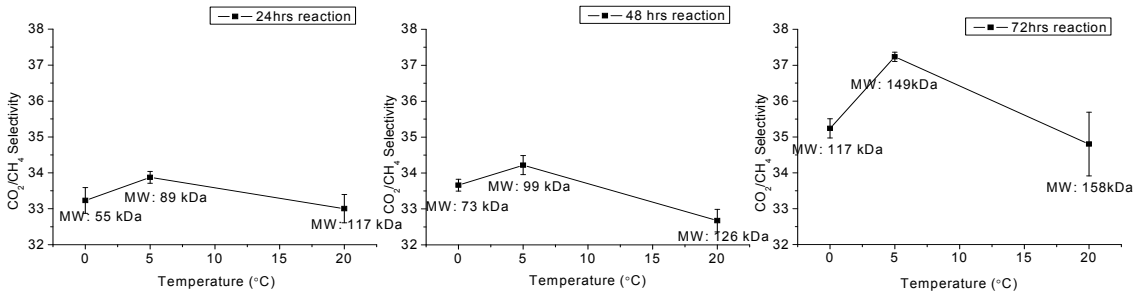

Figure 4.6: Polymerization temperature impact on CO_2/CH_4 selectivity.

As shown in Figure 4.6, given the same polymerization time, selectivity shows a maximum at 5 ℃. Considering only the molecular weight effect, as temperature increases, selectivity should increase due to high molecular weight of PDMC with fewer bypasses. For PDMC polymerized at 20℃, the randomization effect can be more significant or more side reactions can occur, and these possibly contribute to a loss of selectivity.

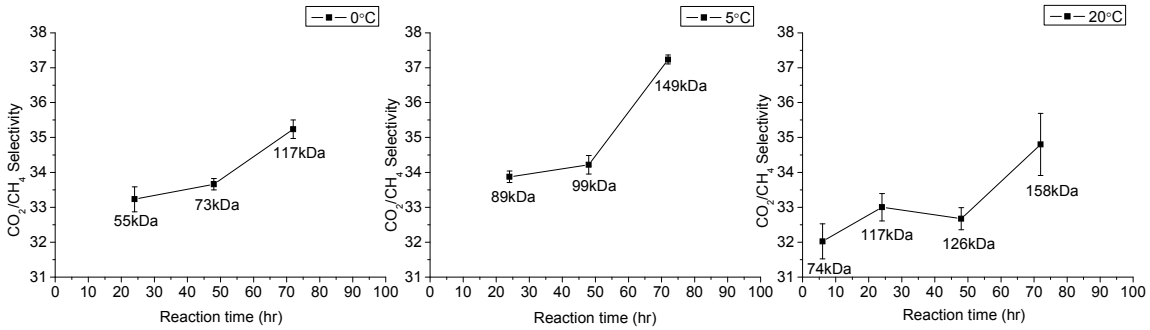

Figure 4.7: Polymerization time impact on CO_2/CH_4 selectivity.

As shown in Figure 4.7, given the same polymerization temperature, as reaction time increases, selectivity increases because higher molecular weight polymer has fewer chain-ends and, hence, lowers free volume [5]. For PDMC polymerized at the same polymerization temperature, the randomization effect is minimal compared to the molecular weight effect even if polymerization time increases. In this case, molecular weight effect is dominant over randomization effect. Thus, the molecular weight effect is at play, and high molecular weight built after sufficient time makes the polymer more selective. PDMC synthesized for only 6 hours at 20℃ show particularly undesirable selectivity due to low molecular weight.

4.4 Effect of polymerization conditions on plasticization suppression

t \ T	0 ℃	5 ℃	20 ℃
6 hr			*7*
24 hr	*1*	*4*	*8*
48 hr	*2*	*5*	*9*
72 hr	*3*	*6*	*10*

t \ T	0 ℃ → 20 ℃
3 hr → 21 hr	*11*

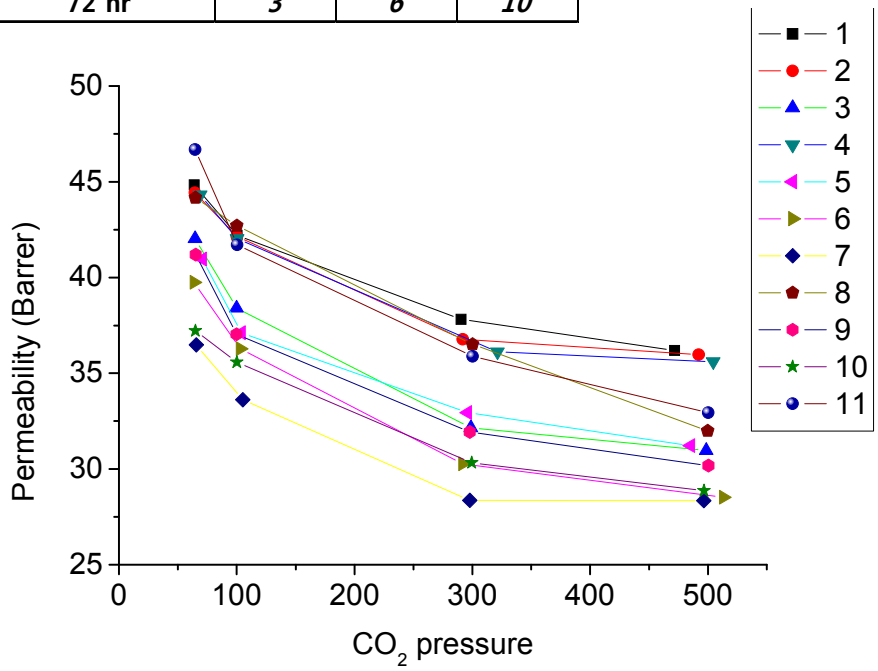

Figure 4.8: Plasticization suppression of *chemically imidized* PDMC. Test conditions: Pure CO_2, CH_4 at 35 ℃.

Interestingly, all the states in the Table 4.1 above show good plasticization suppression up to 500 psi of pure CO_2 at 35 ℃. Successful plasticization stability against high feed pressure suggests that all the states are crosslinked partially or completely. In section 4.5, gel fraction was used as an additional indicator of sufficient stabilization to avoid excessive swelling in aggressive feeds [6]. The gel fraction explains how all the samples synthesized in this study show plasticization suppression.

4.5 Gel fraction test

Table 4.2: Gel fraction of *chemically imidized* PDMC.

t \ T	0 ℃	5 ℃	20 ℃	t \ T	0 ℃ → 20 ℃
6 hr			*7*	3 hr → 21 hr	*11*
24 hr	*1*	*4*	*8*		
48 hr	*2*	*5*	*9*		
72 hr	*3*	*6*	*10*		

	Chem 1	Chem 2	Chem 3	Chem 4	Chem 5	Chem 6	Chem 7	Chem 8	Chem 9	Chem 10	Chem 11
220c 2hr / THF	0.87	0.88	0.91	0.88	0.91	0.95	0.77	0.92	0.92	0.94	0.93

Films crosslinked at 220 ℃ for 2hrs are treated by immersion in THF for two days. Gel fraction is over 90% for most of the states except states 1, 2, 4, and 7 synthesized for insufficient polymerization time. From Figure 4.9, it is noteworthy to check that even incompletely crosslinked PDMC could suppress plasticization at high CO_2 pressure. Of all states, states 6 and 10 showed higher gel fraction about 95%, perhaps because molecular weight of the states are high, and the number of dangling chain ends is low. Generally, gel fraction of most of *chemically imidized* states is relatively high and constant.

4.6 Conclusions

As shown above, as polymerization time increases, molecular weight roughly tends to increase thereby decreasing permeability and increasing selectivity with a few exceptions. As polymerization temperature increases, molecular weight roughly tends to increase thereby decreasing permeability and increasing selectivity with a few exceptions. The exceptions were described above. Most of the states showed decent plasticization suppression up to 500 psi and high crosslinking density after crosslinking at 200 ℃ for 2 hours. Of states from 1 to 11, PDMC from the state 6 seems to be the best in terms of selectivity (approximately 37), plasticization suppression, and crosslinking density. Permeability of the state 6 (approximately 39) is a little bit lower than some other states, the permeability loss will be compensated by doing imidization thermally as you will see in chapter 5.

4.7 References

[1] Takekoshi, T., Polyimides (Wilson, D., hergenrother, P., and Stengenberger, H. ed.), Blackie, Chapman and Hal, NY, 1990.

[2] Koton, M.M., Kudryavtsev, V.V., Sklizkova, V.P., Bessonov, M.I., Smirnova, V.E., Belenky, B.G, and Kolegov, V.I., Zh. Prikl,. Khim., 49(2), 387, 1976.

[3] Wulin Qiu, Chien-Chiang Chen, Liren Xu, Lili Cui, Donald R Paul, W.J. Koros, Sub-Tg Cross-linking of a Polyimide Membrane for Enhanced CO2 Plasticization Resistance for Natural Gas Separation. Macromolecules, 44 (2011), p. 6046.

[4] M. T. Guzman-Gutierrez, M. H. Rios-Dominguez, F. A. RuizTrevino, M. G. Zolotukhin, J. Balmaseda, D. Fritsch and E. Prokhorov, Structure-properties relationship for the gas transport properties of new fluoro-containing aromatic polymers, J. Membr. Sci., 2011, 385–386, 277–284.

[5] Santangelo, P. G., Ngai, K. L., Roland, C. M., Molecular weight dependence of fragility in polystyrene, Macromolecules, 1993, 26, 2682−2687

[6] He. J. H, Horie. K and Yokota. R, Characterization of polyimide gels crosslinked with hexamethylene diisocyanate, 2000, Polymer 41 4793–802

CHAPTER 5

PERFORMANCE OF THERMALLY IMIDIZED PDMC

5.1 Introduction

Chapter 4 discusses optimization of polymer properties and transport properties of *chemically imidized* PDMC polyimide. This chapter contains gas separation performance of PDMC polyimide synthesized using *thermal imidization*. Polyamic acid of *thermally imidized* PDMC was synthesized using the state 6. FTIR, TGA, XRD, DSC, DMA, and NMR characterized both thermally imidized PDMC polyimide and *chemically imidized* PDMC polyimides.

5.2 Gas permeation

5.2.1 Pure gas permeation

Table 5.1: Pure gas permeation data of this work and literature [1-3].

	Test pressure	Test gas	CO2 Permeability	CO_2/CH_4 Selectivity	Crosslinking conditions / MW	Imidization method
Ma	65 psia	Pure gas	34 Barrer	36	200°C, 2 hrs /120k	Chemical
This study	65 psia	Pure gas	39 Barrer	37	200°C, 2 hrs / 150K	Chemical
Ward	65 psia	Pure gas	67 Barrer	34	200°C, 2 hrs / 150K	Thermal
Hillock	65 psia	Pure gas	58 Barrer	37	220°C, 24 hrs / 42k	Thermal
This study	65 psia	Pure gas	64 Barrer	34	200°C, 2 hrs / 150K	Thermal

In pure gas permeation with pure CO_2 and CH_4 at 65psi, thermally imidized PDMC (MW: 150K) synthesized in this study show similar gas transport properties (permeability: 63 Barrers, CO_2/CH_4 selectivity: 34) with Hillock' thermally imidized PDMC (permeability: 58 Barrers, CO_2/CH_4 selectivity: 37) and Ward's thermally imidized PDMC (permeability: 67 Barrers, CO_2/CH_4 selectivity: 34). Surprisingly,

thermally imidized PDMC show 70% higher permeability than *chemically imidized* PDMC without sacrificing selectivity much.

The significant increase in permeability of thermally imidized PDMC could arise from one or both of two factors. The first possibility is that monomers form different kinds of bonds due to high temperature during thermal imidization. Conducting FTIR and NMR could test the first hypothesis. A second possibility is that different monomer sequence distribution leads to change free volume fraction of *chemically imidized* PDMC and thermally imidized PDMC. TGA, XRD, DSC, and DMA could verify the second hypothesis. Three repetitive pure gas permeation tests were conducted with separate samples to confirm the reproducibility of permeability of both *chemically imidized* polymer and thermally imidized polymer.

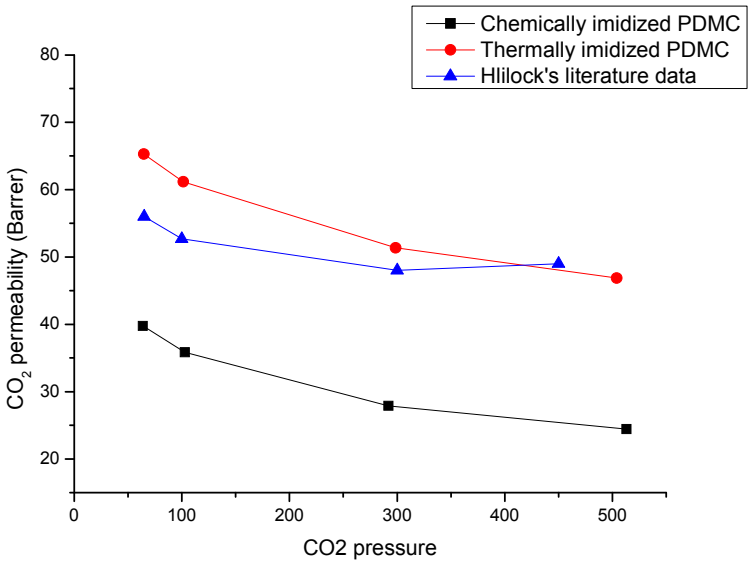

Figure 5.1: Plasticization suppression of *chemically imidized* PDMC in this work, thermally imidized PDMC in this work, and Hillock's *thermally imidized* PDMC. Test conditions: Pure CO_2, CH_4 at 35℃ [3].

As shown in Figure 5.1, *thermally imidized* PDMC was also tested up to high feed pressure 500 psi of pure CO_2 and CH_4 to check whether it shows sufficient

plasticization suppression. It was found that *thermally imidized* PDMC show similar plasticization suppression as seen for *chemically imidized* PDMC showed up to 500 psi for pure CO_2 at 35℃.

5.2.2 Mixed gas permeation

In mixed gas permeation with 10/90 CO_2/CH_4 at 200psi, thermally imidized PDMC synthesized in this study show similar gas transport properties (permeability: 77 Barrers, CO_2/CH_4 selectivity: 45) with Ward's thermally imidized PDMC (permeability: 80 Barrers, CO_2/CH_4 selectivity: 46) [2]. *Chemically imidized* PDMC synthesized in this study show similar gas transport properties (permeability: 60 Barrers, CO_2/CH_4 selectivity: 46) with Ma's *chemically imidized* PDMC (permeability: 57 Barrers, CO_2/CH_4 selectivity: 45) [1]. For mixed gas permeation, thermally imidized PDMC show approximately 30% higher permeability than chemically imidized PDMC. Besides, both thermally imidized PDMC and *chemically imidized* PDMC demonstrate a good agreement with previous researchers' data. Permeability and selectivity is significantly more pronounced in the feed containing 10/90 CO_2/CH_4 relative to the pure gas feed. The above data of permeation and selectivity confirmed again that permeability of thermally imidized PDMC is higher than that of *chemically imidized* PDMC without sacrificing selectivity much.

5.3 FTIR analysis of Imidization methods

Both thermally imidized polymer and *chemically imidized* polymer were further characterized by FTIR. FTIR measurements showed no significant structural difference. Das did FTIR characterization on *chemically imidized* 6FDA-6FpDA and thermally imidized 6FDA-6FpDA, and they did not differ in FTIR [4].

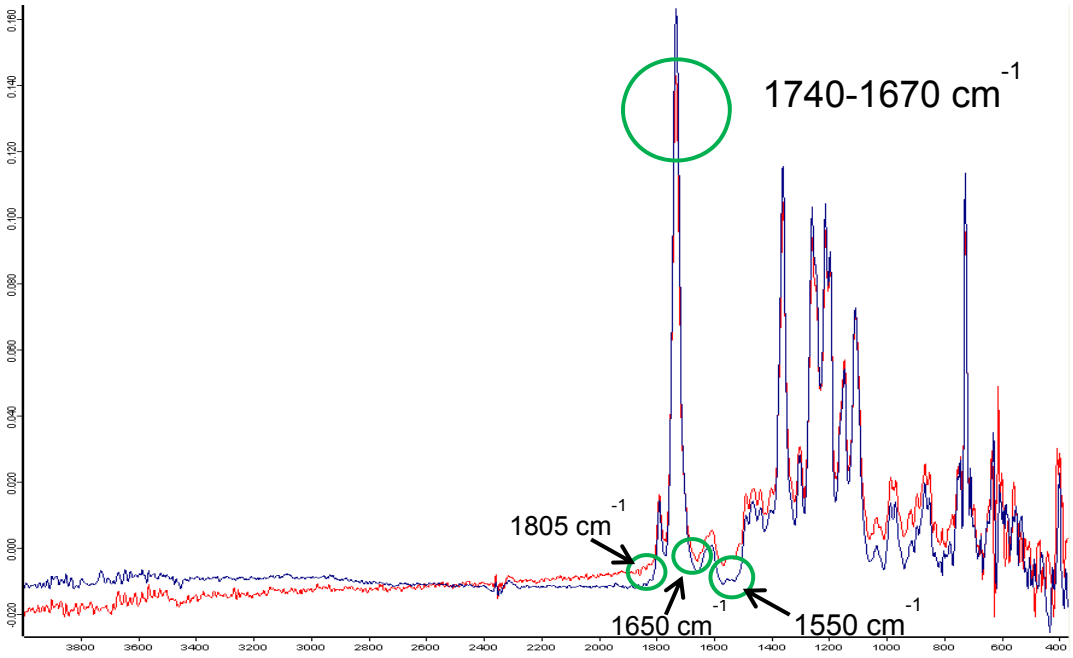

Figure 5.2: FTIR results of *chemically imidized* 6FDA-DAM:DABA (3:2) and *thermally imidized* 6FDA-DAM:DABA(3:2).

Amides typically show an absorption at 1695-1630 cm^{-1} associated with C=O stretching and an absorption at 1550 cm^{-1} associated with H-N-C bond bend stretching. On the other hand, cyclic imides exhibit a strong band at 1740-1670 cm^{-1} [5]. As shown in Figure 5.2, a strong peak at 1740-1670 cm^{-1} exist in both *chemically imidized* 6FDA-DAM:DABA (3:2) and *thermally imidized* 6FDA-DAM:DABA (3:2), and there are no peaks in the spectrum at 1650 cm^{-1} and 1550 cm^{-1}. Based on these data, both *chemically* and *thermally imidized* 6FDA-DAM:DABA (3:2) appear to have completed the imidization reaction. We also considered whether side reactions such as isoimide formation could occur during the chemical imidization, however, the results indicate that there is no detectable side reaction. A characteristic isoimide peak at 1805 cm^{-1} due to anhydride groups was not shown in FTIR results.

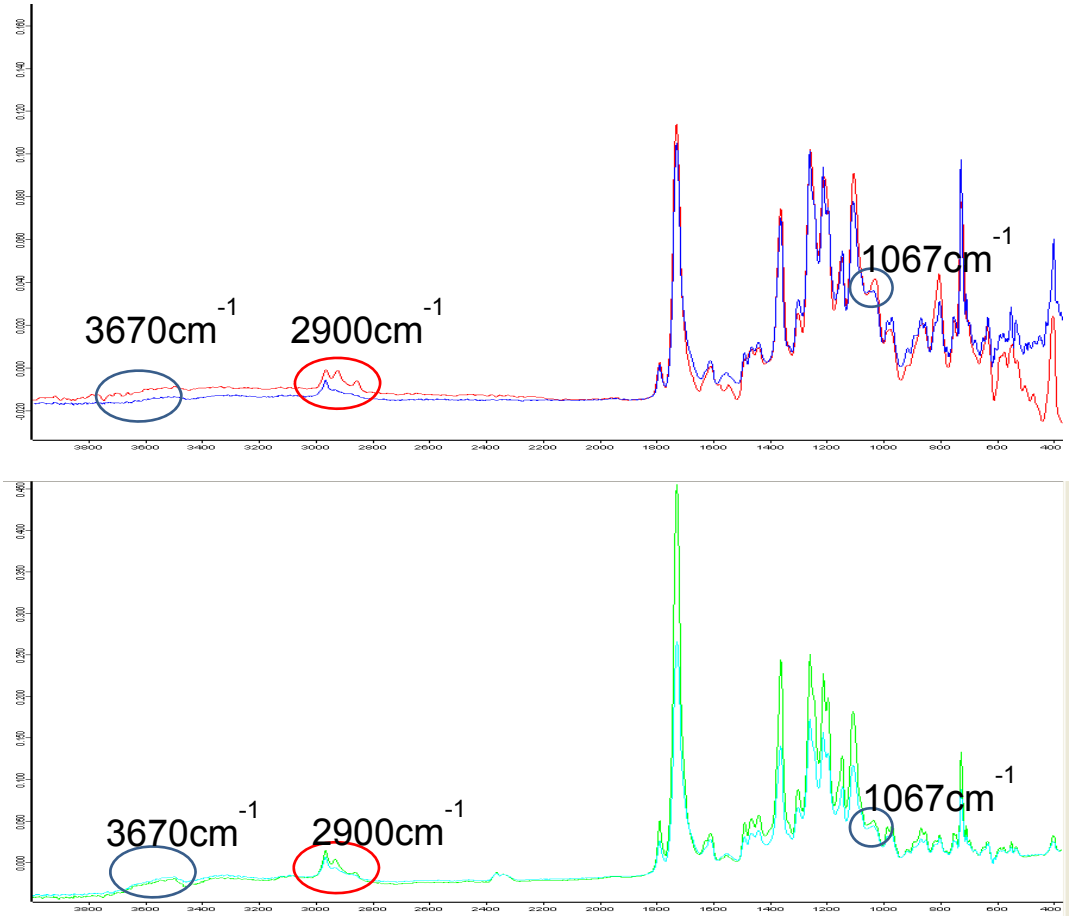

Figure 5.3: FTIR results of chemically imidized uncrosslinked PDMC and *thermally imidized* uncrosslinked PDMC [above] and chemically imidized crosslinked PDMC and *thermally imidized* crosslinked PDMC [below].

Wallace reported that at 180° C for 3 hours, 69% of the possible crosslinking has occurred, while at 200 °C for three hours, completion has reached 73% [6]. In this study, both types (thermal and *chemically imidized*) PDMC were crosslinked at 200°C for 2 hours, so partially incomplete crosslinking might occur. Despite incomplete crosslinking, the crosslinking temperature 200 °C has been used for subsequent hollow fiber application because hollow fiber structure could collapse at temperature above 200 °C [7]. As shown in Figure 5.3, in both uncrosslinked PDMC and crosslinked PDMC, peaks at 3670 cm^{-1}, 2900 cm^{-1} and 1067 cm^{-1} exist. As shown in Table 5.2, among the peaks, a peak 2900 cm^{-1} is present in propanediol and NMP,

but peaks 3670 cm^{-1} and 1067 cm^{-1} exist only in propanediol. After esterification, peaks 3670 $cm^{-1}$and 1067 cm^{-1} appear. Integration of areas under peaks 3670 $cm^{-1}$and 1067 cm^{-1} suggests that both peaks diminished after crosslinking [6]. However, both peaks exist in the crosslinked PDMC because as discussed above, crosslinking does not occur fully at 200 °C. Since FTIR results are not quantitative, only qualitative analysis can be done in this work.

Table 5.2: Source of three peaks 3670 cm^{-1}, 2900 cm^{-1} and 1067 cm^{-1} [6].

Frequency (cm^{-1})	Stretch	Source
3670	O-H	Propanediol
2900	C-H	Propanediol+NMP
1067	C-O	Propanediol

5.4 NMR analysis of Imidization methods

Chemically imidized 6FDA-DAM:DABA (3:2) and *thermally imidized* 6FDA-DAM:DABA (3:2) were further characterized by NMR analysis.

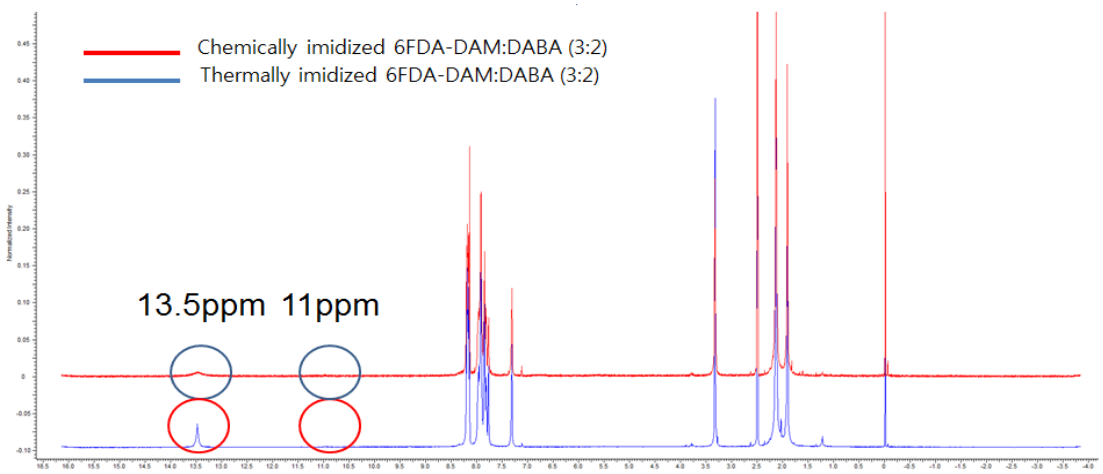

	Chemically imidized 6FDA-DAM:DABA(3:2)	Thermally imidized 6FDA-DAM:DABA(3:2)
DAM:DABA ratio	1.50	1.50
Imidization yield	100%	100%
Esterification yield	0%	0%

Figure 5.4: ^{1}H NMR results of *chemically imidized* 6FDA-DAM:DABA (3:2) and *thermally imidized* 6FDA-DAM:DABA(3:2).

The imidized 6FDA-DAM:DABA (3:2) samples do not differ significantly in NMR analysis between chemical and thermal imidization routes . The intensity of a peak located at 13.5ppm (-COOH group) seems slightly different, but areas below the peak are the same. [8] If both 6FDA-DAM:DABA (3:2) are completely imidized, peaks appear only from the –COOH group of DABA moieties, and areas should be the same.

Ratio between 6FDA-DAM and 6FDA-DABA is close to 1.5. The ratio should be strictly close to 1.5 to achieve high molecular weight 6FDA-DAM:DABA (3:2). A

small stoichiometric deviation reduces the chance of achieving high molecular weight significantly.

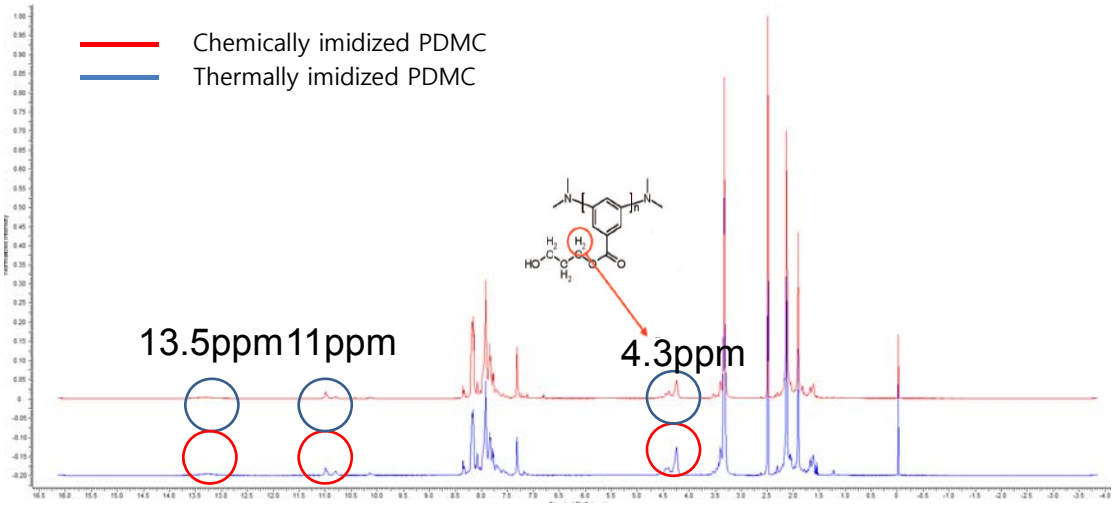

	Chemically imidized PDMC	Thermally imidized PDMC
DAM:DABA ratio	1.52	1.51
Imidization yield	80%	89%
Esterification yield	173%	105%

Figure 5.5: ^{1}H NMR results of uncrosslinked *chemically imidized* PDMC and *thermally imidized* PDMC.

A peak at 11ppm is considered as –NH-, and imidization yield was calculated based on the intensity of peak at 11ppm [8]. Both 6FDA-DAM:DABA (3:2) turn out to be completely imidized prior to crosslinking.

Despite being completely imidized before crosslinking, imidization yield of both PDMC appears to be below 100% because ring opening took place during the esterification. As shown in Figure 5.5, Omole reported that at the esterification temperature 130℃, there could be opening of rings due to small amount of hydrolysis, but the primary backbone does not break. [9] As Omole said, molecular weight breakdown was not observed during the esterification in this work. The reason esterification yield is higher than 100% is because a few rings open partially. Once a

ring opens, additional –COOH groups appear and provide crosslinking sites which will be subsequently esterified by 1,3–propanediol. The partial ring opening does not affect molecular weight measurably, since the fundamental backbone is not hydrolyzed during thermal imidization. As shown in Figure 5.5, at 4.3 ppm, a new kind of peak appeared after esterification. The peak at 4.3 ppm is due to the first two hydrogens of 1,3-propanediol, so the peak can be used to calculate the esterification yield. In conclusion, since there is no significant chemical structure difference between *chemically imidized* PDMC and *thermally imidized* PDMC, difference of transport properties might be mainly due to monomer sequence distribution.

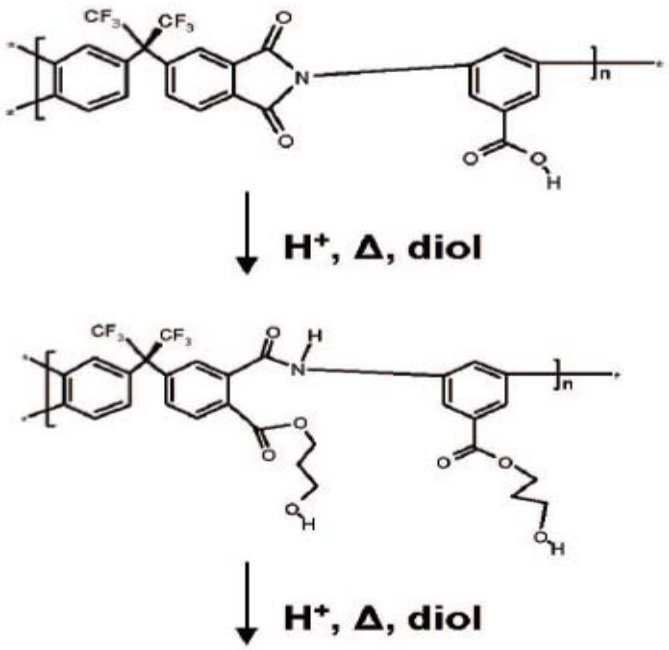

.

Figure 5.6: Partial ring opening of PDMC [9].

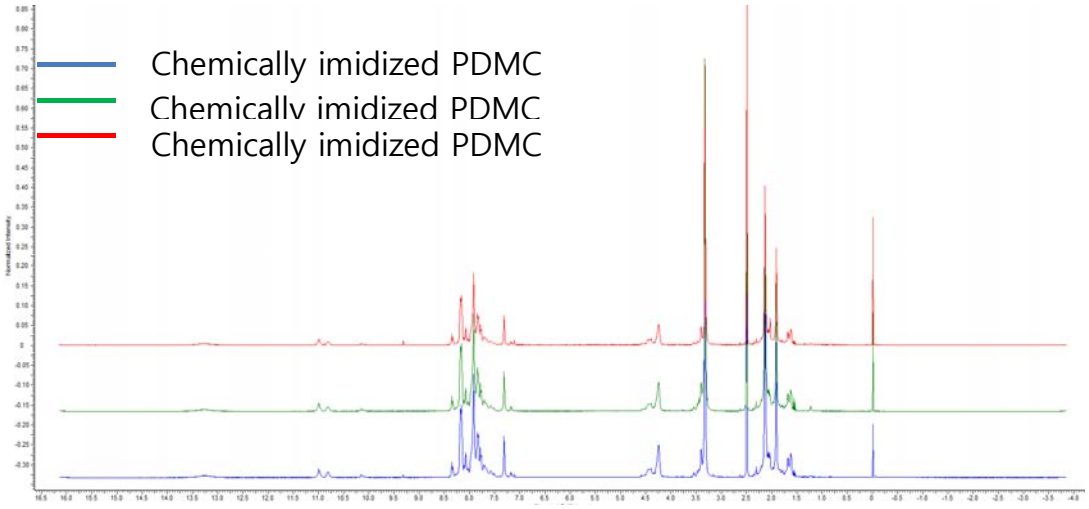

Figure 5.7: Comparison of NMR results of chemically imidized PDMC #3, #6, and #10.

Chemically imidized PDMC polymerized for 72 hours is analyzed by NMR. Polymerization temperatures are 0℃, 5℃, and 20℃ respectively. Surprisingly, the three NMR results are very close to each other, which indicate that there was no significant side reaction to affect transport properties and molecular weight. This observation shows that concerns that there might be side reactions during imidization at high temperature (20℃) are not valid. By ruling out the possibility of side reaction, we conclude that the difference of transport properties might be explained by monomer sequence distribution.

5.5 TGA analysis of Imidization methods

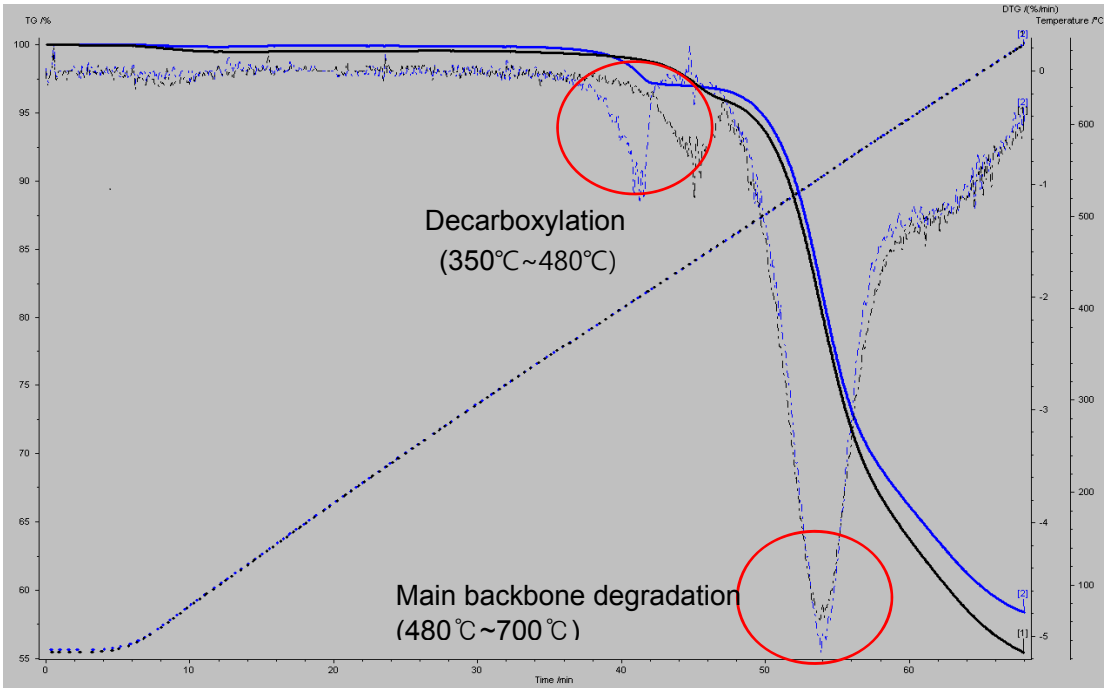

Figure 5.8: TGA traces of *chemically imidized* 6FDA-DAM:DABA (3:2) and *thermally imidized* 6FDA-DAM:DABA (3:2).

Figure 5.8 shows the TGA traces of imidized 6FDA-DAM:DABA (3:2) polymers. Weight loss below 320℃ is due to the evaporation of solvents and water sorbed in the polymer. Prior to main backbone degradation initiating at about 480 ℃, both *chemically imidized* and thermally imidized 6FDA-DAM:DABA (3:2) show a minor weight loss about 3.2 wt% from 350 ℃ to 480 ℃, which is attributed to the decarboxylation of -COOH groups of DABA moieties and partial degradation of the resulting polyimide (theoretical weight loss due to decarboxylation is 3.3 wt%). Qiu

proved that the minor weight loss from 350℃-480℃ is only due to decarboxylation of DABA moieties by comparing TG-MS (Thermogravimetric analysis–mass spectrometry) traces of 6FDA-DAM, *6*FDA-DABA, and 6FDA-DAM:DABA(3:2). [7] Interestingly, the maximum peak of *chemically imidized* 6FDA-DAM:DABA (3:2) due to decarboxylation located at 420℃ while the maximum peak of *thermally imidized* 6FDA-DAM:DABA (3:2) due to decarboxylation is located at 460℃. As shown in Figure 5.9, the decarboxylation mechanism starts from anhydrides formation from –COOH groups of DABA moieties. Upon further heating, these anhydrides have been shown to release CO_2 [10-11].

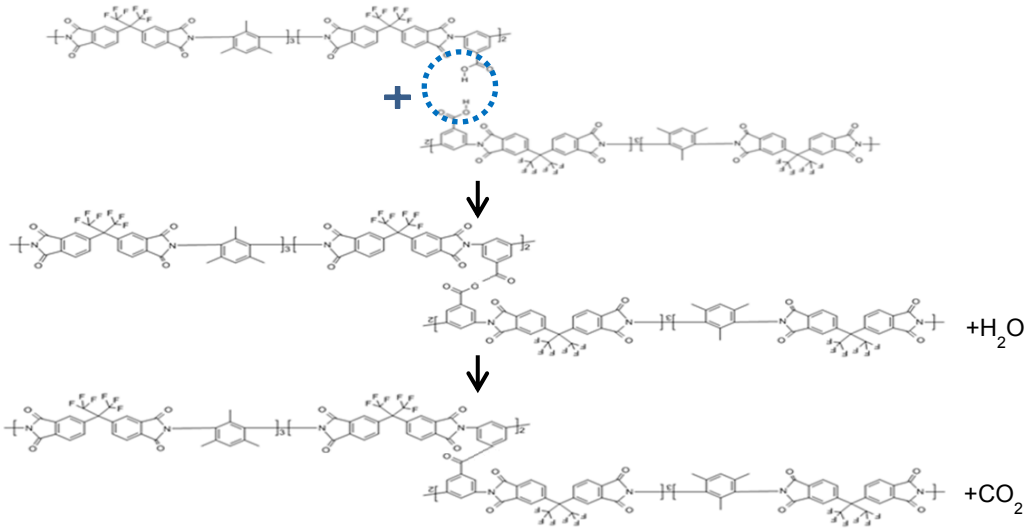

Figure 5.9: A Decarboxylation mechanism.

Three bulky methyl groups of DAM monomers might sterically hinder anhydrides formation from –COOH groups of DABA monomers, thereby increasing decarboxylation temperature as you can see from Figure 5.10. This result suggests that intermolecular steric hindrance of DAM moieties might explain differences between the decarboxylation temperature of *thermally imidized* 6FDA-DAM:DABA (3:2) and that of *chemically imidized* 6FDA-DAM:DABA (3:2).

a) Thermally imidized 6FDA-DAM:DABA (3:2)

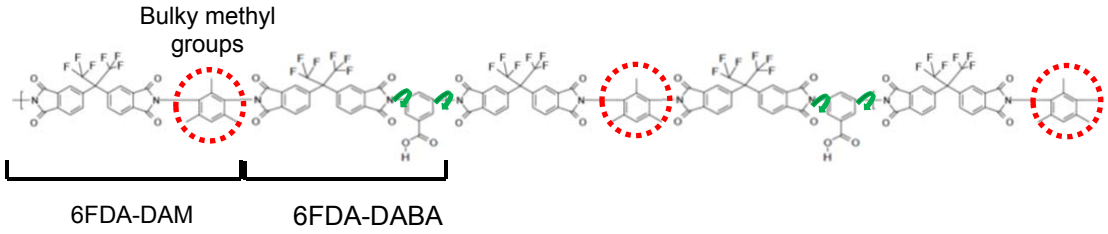

b) Chemically imidized 6FDA-DAM:DABA (3:2)

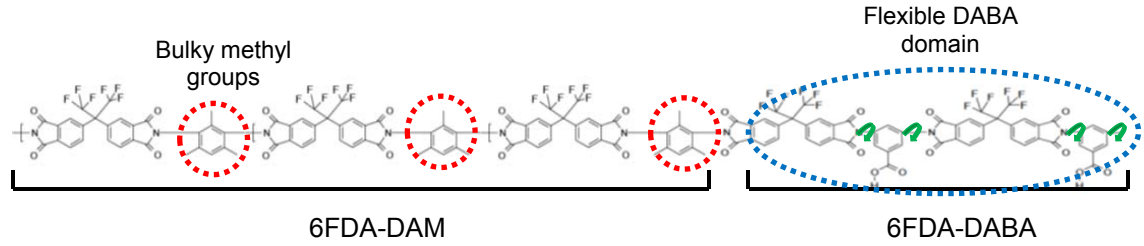

Figure 5.10: a) Thermally imidized 6FDA-DAM:DABA(3:2) with less flexible DABA moieties b) Chemically imidized 6FDA-DAM:DABA(3:2) with more flexible DABA domain

The hindrance of three methyl groups on DAM monomers is hypothesized to be not so important in *chemically imidized* 6FDA-DAM:DABA (3:2), since *chemically imidized* 6FDA-DAM:DABA (3:2) is believed to give rise to less randomized copolymers. Less randomized chains contain more flexible DABA domains which are able to approach easily to each other for decarboxylation. On the other hand, in thermally imidized 6FDA-DAM:DABA (3:2), it is believed that 6FDA-DAM and 6FDA-DABA moieties are more randomly distributed, thereby increasing the local steric hindrance effects between 6FDA-DAM and 6FDA-DABA moieties. Uniformly dispersed 6FDA-DAM moities could restrict rotational motions of significant segments of the chains, hence making it more difficult for DABA moieties to approach to each other, thereby possibly increasing decarboxylation temperature.

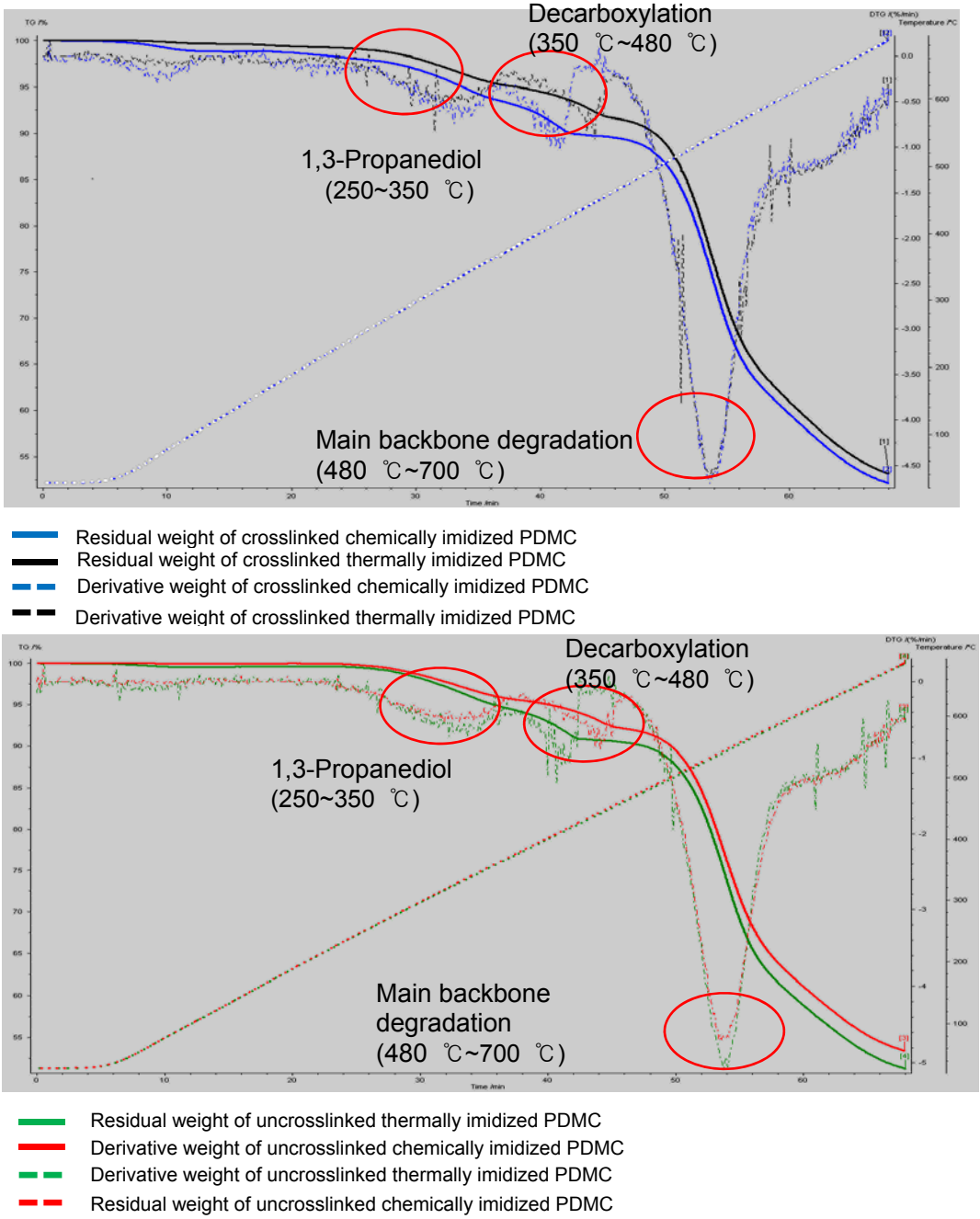

Figure 5.11: TGA traces of uncrosslinked PDMC (above) and crosslinked PDMC (below).

As shown in Figure 5.11, there was no significant difference between crosslinked PDMC and uncrosslinked PDMC TGA results. PDMC samples show three weight loss peaks in derivative weight curve. The first weight loss starting at

about 250℃ was caused by the small amount of 1,3-propanediol removed during the transesterification process (See Appendix C). As Wallace reported, crosslinking at 200℃ for 2 hours could not achieve 100% crosslinking, both uncrosslinked PDMC and crosslinked PDMC should have a small unreacted portion of 1,3-propanediol which is able to crosslink during the TGA test. Since the amount of crosslinking during TGA test (20 minutes) is small, the amount of removed 1,3-propanediol in the transesterification process, through which the polyimide is crosslinked during TGA test, should be almost the same in both uncrosslinked PDMC and crosslinked PDMC. The second weight loss was caused by decarboxylation of unreacted –COOH groups. The third primary weight loss was caused by the decomposition of polymer main chains. The existence of the second weight loss in derivative weight curve of uncrosslinked PDMC suggests that partial monoesterification of –COOH groups occurs during the TGA study. Specifically, completely monoesterified PDMC, which all of the -COOH groups reacted with 1,3-propanediol would show only two weight losses, so the weight loss caused by unreacted –COOH groups should disappear. In any case, this small amount of uncrosslinked units must be tolerated to avoid morphology collapse when the PDMC material is ultimately used in an asymmetric fiber.

5.6 DSC analysis of Imidization methods

	M_n	M_w	DAM:DABA	Imidization method	Glass transition temperature (T_g)
Wind	Unknown	Unknown	2:1	Chemical	358℃
This study	44K	115K	3:2	Chemical	383℃
Kim	38K	73K	2:1	Thermal	376℃
Kratochvil	78K	150K	2:1	Thermal	374℃
This study	46K	118K	3:2	Thermal	388℃

At the beginning of this work, I noted that *chemically imidized* polymers might be close to a block copolymer and show two distinctive T_g: 382℃ for 6FDA-DAM and 348℃ for 6FDA-DABA respectively. However, previous researchers showed only one T_g, which indicates that *chemically imidized* 6FDA-DAM:DABA is not completely a block copolymer. Now, I hypothesize that both thermal and chemical cases are random to some degree; however, the degree of randomness of monomer sequences may be higher in thermal cases. As shown in Table 5.3, T_g of *thermally imidized* 6FDA-DAM:DABA (2:1) is higher than that of *chemically imidized* 6FDA-DAM:DABA(2:1). Likewise, in this study, the T_g of *thermally imidized* 6FDA-DAM:DABA (3:2) is higher than that of *chemically imidized* 6FDA-DAM:DABA(3:2). (T_g of Polymers whose M_n above 25K typically do not depend significantly on molecular weight much [16]) Due to the high temperature (~190℃) of thermal imidization, both *thermally imidized* 6FDA-DAM:DABA and PDMC are expected to have more or less random monomer sequences. As monomer sequences randomize, three bulky CH_3- groups of DAM monomers might inhibit rotation of neighboring DABA monomers more significantly, thereby increasing the glass transition temperature. Also, in a thermal case, the increased spacing between carboxylic acid groups of DABA moieties could provide optimized hydrogen bonding, which

consequently could make the glass transition temperature higher [12]. However, steric hindrance seems to be a more important factor than hydrogen bonding effect in this work. If hydrogen bonding effect were dominant, then T_g of 6FDA-DABA should be higher than T_g of 6FDA-DAM since only 6FDA-DABA can form hydrogen bonding through carboxylic acid groups. However, literature reports the opposite [7]. In addition, 6FDA-mPDA which lack carboxylic acid groups and bulky three methyl groups showed the lowest T_g, and the order of T_g was reported to be 6FDA-mPDA<6FDA-DAM<6FDA-DABA [7]. After all, a steric hindrance seems to be a dominant factor to contribute to T_g increase of 6FDA-DAM:DABA (3:2) in this work.

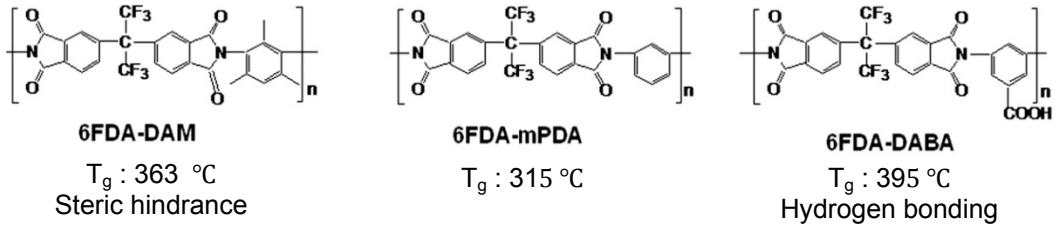

Figure 5.12: T_g of 6FDA-DAM, 6FDA-mPDA and 6FDA-DABA [7].

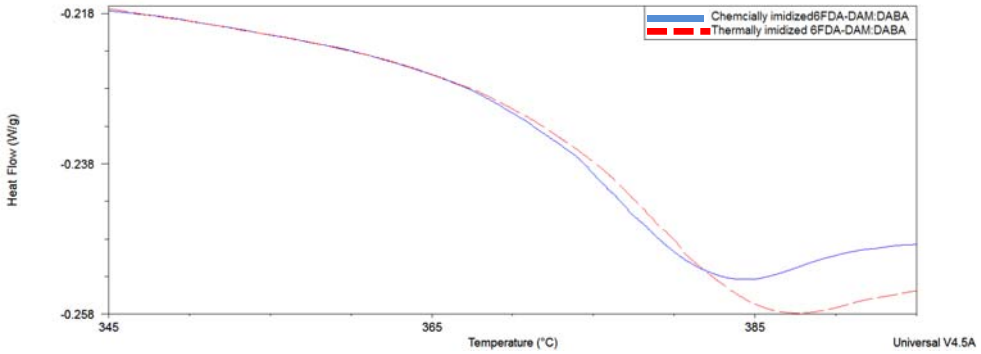

Figure 5.13: DSC results of *chemically imidized* 6FDA-DAM:DABA (3:2) and *thermally imidized* 6FDA-DAM:DABA (3:2). T_g of *chemically imidized* PDMC: 383 ± 1℃, T_g of *thermally imidized* PDMC: 388 ± 1℃.

As shown in Figure 5.13, *thermally imidized* 6FDA-DAM:DABA (3:2) showed

a higher glass transition temperature (T_g), presumably because of randomized monomer sequence.

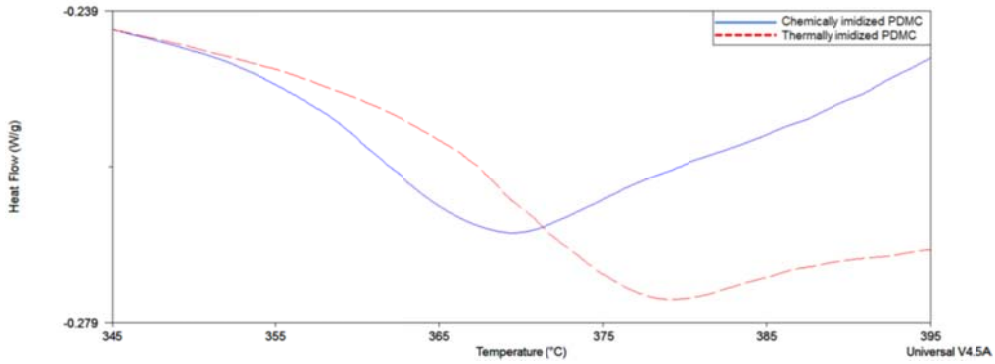

and
zed

As shown in Figure 5.14, in similar way with 6FDA-DAM:DABA (3:2), crosslinked *thermally imidized* PDMC showed higher glass transition temperature (T_g) because of randomized monomer sequence. The difference of T_g in 6FDA-DAM:DABA (3:2) and crosslinked PDMC could support that degree of randomization of monomer sequences differ in chemical and thermal cases.

5.7 DMA analysis of Imidization methods

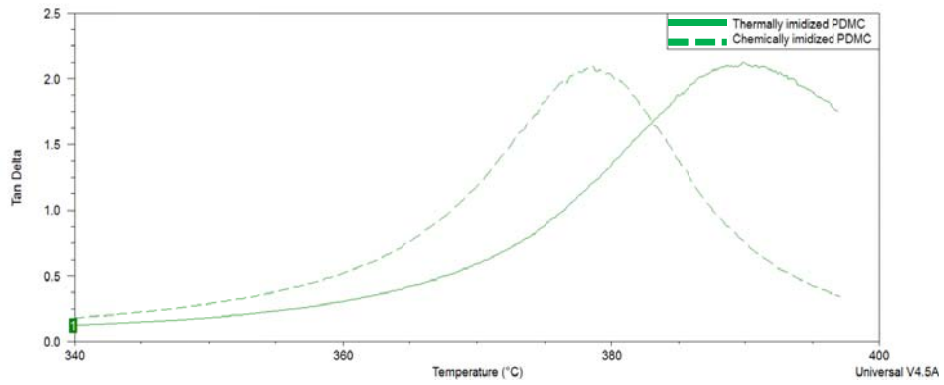

lized
)MC:

In DMA data, maximum of modulus peak is located at the glass transition temperature (T_g). As shown in DSC data, *chemically imidized* polymer (presumably less randomized copolymer) is expected to show lower T_g than thermally imidized polymer (more randomized copolymer). For a given sample, DMA produces higher T_g values than DSC due to the nature of the measurement [17]. The T_g from DMA was obtained by the maximum of the peak of tan delta. From DMA, the T_g of *chemically imidized* PDMC is 378℃ and T_g of *thermally imidized* PDMC: 390℃(From DSC, T_g of *chemically imidized* PDMC is 367℃ and T_g of *thermally imidized* PDMC: 378℃.) DMA also seems consistent with the hypothesis that the monomer sequences of *thermally imidized* PDMC maybe more randomized, thus show higher T_g.

5.8 XRD analysis of Imidization methods

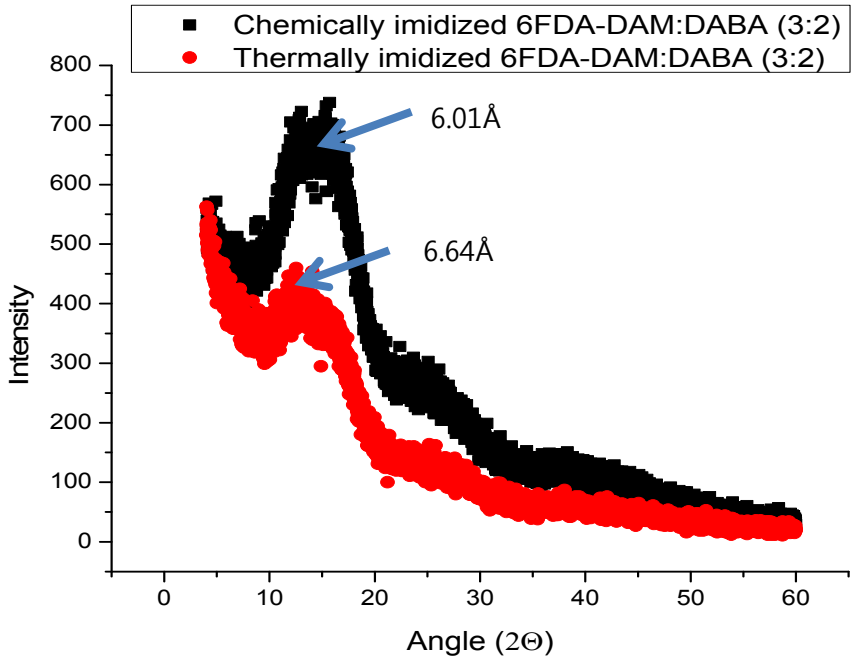

Figure 5.16: XRD results of *chemically imidized* 6FDA-DAM:DABA (3:2) and *thermally imidized* 6FDA-DAM:DABA (3:2).

In XRD data, using Bragg's law, the average spacing of amorphous polymer is calculated using the Bragg's law. Bragg's law can be expressed by $n\lambda = 2d\sin\theta$, in which n is an integer, λ is the wavelength of incident x-ray, d is the spacing between the planes in the atomic lattice, and 2θ is the angle between the incident ray and the scattering planes. Although d-spacing could not be used as a true inter-chain distance, the increased average inter-chain spacing in amorphous polymer is correlated with the free volume and permeability of polyimides [18]. An increase in permeability of *thermally imidized* 6FDA-DAM:DABA (3:2) is consistent with the wide-angle X-ray diffraction patterns. *Thermally imidized* and *chemically imidized* 6FDA-DAM:DABA (3:2) shows 6.64 Å and 6.01 Å, respectively. Since molecular weight could affect the average spacing, molecular weight of both imidized 6FDA-DAM:DABA (3:2) samples used should be approximately the same (~110 kDa).

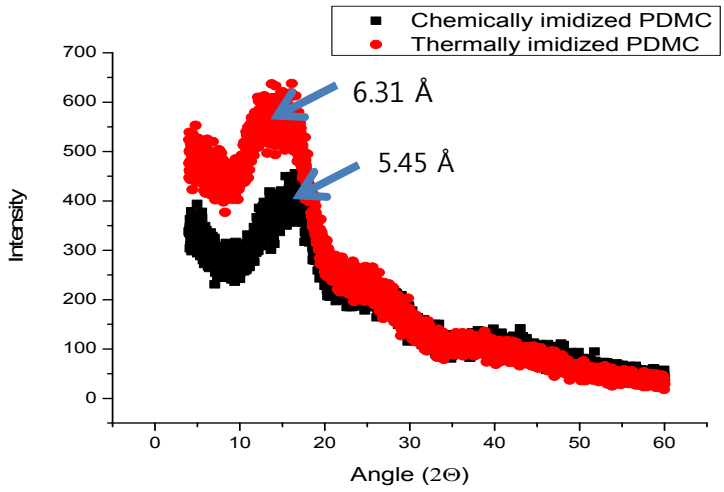

Figure 5.17: XRD results of *chemically imidized* PDMC and *thermally imidized* PDMC.

An increase in permeability of *thermally imidized* 6FDA-DAM:DABA (3:2) is also consistent with the wide-angle X-ray diffraction patterns as well. *Thermally*

imidized 6FDA-DAM:DABA (3:2) shows 6.31 Å and *chemically imidized* 6FDA-DAM:DABA (3:2) show 5.45 Å. Since molecular weight could affect the average spacing, molecular weight of both imidized 6FDA-DAM:DABA (3:2) samples used should be approximately the same (~150 kDa).

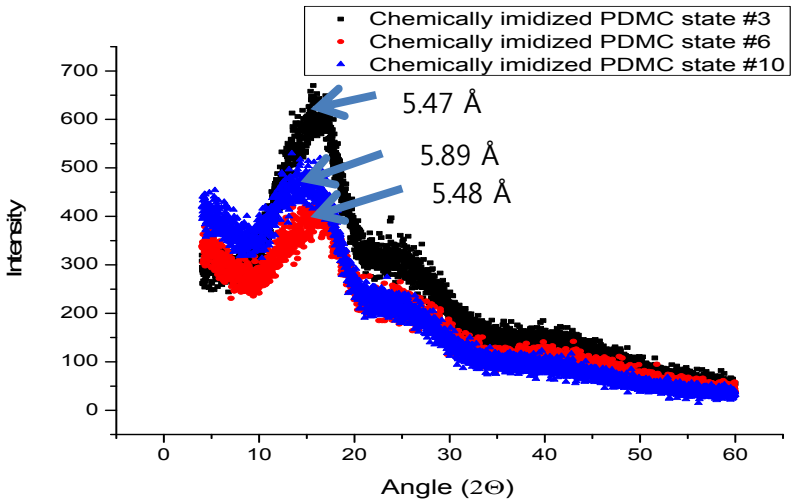

Figure 5.18: XRD results of chemically imidized PDMC #3, #6, and #10.

States 3, 6, and 10 are PDMC polymerized for 72 hours at different temperatures (0℃, 5℃, and 20℃). As discussed in Section 4.2 and 4.3, since kinetics is dominant over thermodynamics, apparently PDMC polymerized at 20℃ should have the highest molecular weight, the lowest d-spacing among them. However, d-spacing of the state 10 turns out to be marginally higher than others, which suggests that at polymerization temperature 20℃, randomization effect may be significant. While the results are similar, we do seem to find trends that may be outside the experimental uncertainty.

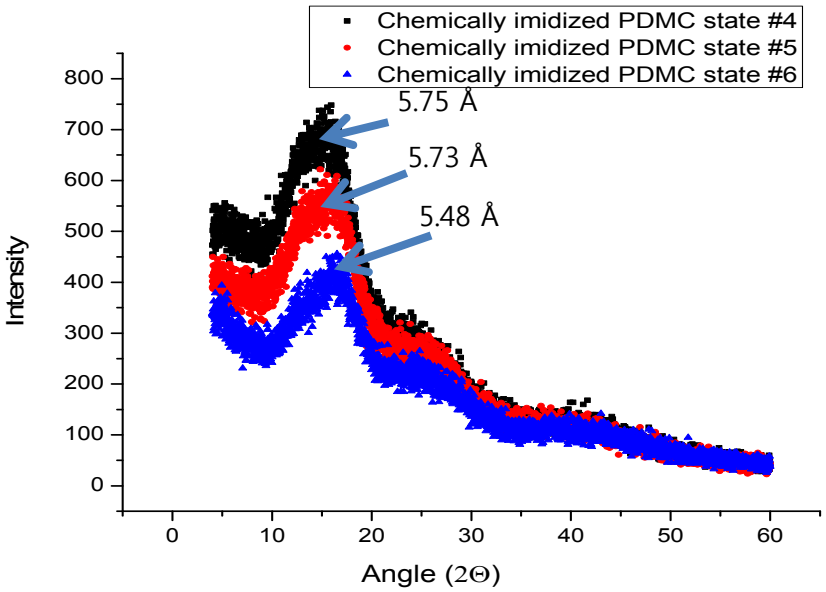

Figure 5.19: XRD results of chemically imidized PDMC #4, #5, and #6.

States 4, 5, and 6 are PDMC polymerized at 5℃ for different polymerization time (24hrs, 48hrs, and 72hrs). As discussed in Section 4.2 and 4.3, since conversion increases as polymerization time increases, apparently PDMC polymerized for 72hrs should have the highest molecular weight, the lowest d-spacing among them.

5.9 Gel fraction test and dissolution test

Gel fraction test of *thermally imidized* PDMC was done following the procedure described in section 3.3.10 because crosslinking density of *thermally imidized* PDMC must reach a certain standard as well. As shown in Table 5.4, crosslinking density of *thermally imidized* PDMC was 0.95 and was comparable to that of *chemically imidized* PDMC.

Table 5.4: Gel fraction of *chemically imidized* PDMC and *thermally imidized* PDMC.

t \ T	0 ℃	5 ℃	20 ℃	t \ T	0 ℃ → 20 ℃
6 hr			*7*	3 hr → 21 hr	*11*
24 hr	*1*	*4*	*8*		
48 hr	*2*	*5*	*9*		
72 hr	*3*	*6*	*10*		

	Chem 1	Chem 2	Chem 3	Chem 4	Chem 5	Chem 6	Chem 7	Chem 8	Chem 9	Chem 10	Chem 11	Thermal
220c 2hr / THF	0.87	0.88	0.91	0.88	0.91	0.95	0.77	0.92	0.92	0.94	0.93	0.95

A dissolution test was done by dissolving PDMC in NMP. Das reported that *thermally imidized* 6FDA-6FPDA may form precipitate in the dope. Das discussed that the precipitate formed chemical crosslinks between the polymer and dehydrating agent, and the precipitate could affect the solubility and spinnability of polymers. [4]

In this work, however, both *thermally imidized* 6FDA-DAM-DABA and PDMC showed no precipitate in solution at all as shown in Figure 5.19. Therefore, no hurdle seems to exist to extend *thermally imidized* PDMC to fiber spinning.

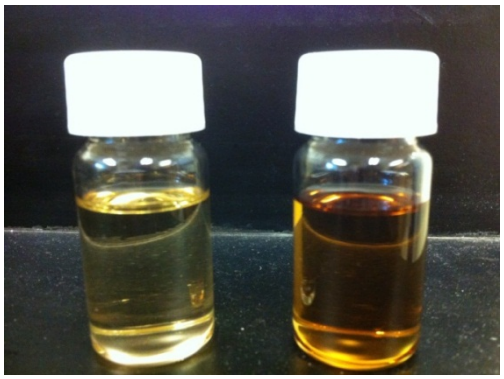

Figure 5.20: Dissolution test (Left: *chemically imidized* PDMC dissolved in NMP, Right: *thermally imidized* P DMC dissolved in NMP)

5.10 Conclusion

Chemically imidized and thermally imidized PDMC showed similar transport properties to data from literatures. Both Chemically imidized and thermally imidized PDMC showed decent plasticization suppression up to 500psi of pure CO_2. NMR and IR data proved that chemical structures of the both PDMC are almost identical to each other. However, transport properties, TGA, DSC, DMA, and XRD suggested that degree of randomization of monomer sequences may differ in chemically imidized PDMC and thermally imidized PDMC. In addition, gel fraction test and dissolution test indicated that both PDMC could be applicable to hollow fiber application.

5.11 Reference

[1] C. Ma, Highly Productive Ester Crosslinkable Composite Hollow Fiber Membranes for Aggressive Natural Gas Separations, Ph.D. Dissertation, in: School of Chemical and Biomolecular Engineering, Georgia Institute of Technology, Atlanta, GA, 2011.

[2] J.K. Ward, CROSSLINKABLE MIXED MATRIX MEMBRANES FOR THE PURIFICATION OF NATURAL GAS, PhD Dissertation, in: School of Chemical & Biomolecular Engineering, Georgia Institute of Technology, Atlanta, GA, 2010.

[3] A.M.W. Hillock, W.J. Koros, Cross-linkable polyimide membrane for natural gas purification and carbon dioxide plasticization reduction, Macromolecules, 40 (2007) 583-587.

[4] M. Das, MEMBRANES FOR OLEFIN/PARAFFIN SEPARATIONS, PhD Dissertation, in: School of Chemical & Biomolecular Engineering, Georgia Institute of Technology, Atlanta, GA, 2009.

[5] Colthup, N. B., Daly, L. H., Wiberley, S. E., Introduction to Infrared and Raman Spectroscopy, San Diego: Academic Press Inc. (1990).

[6] D.W. Wallace, Crosslinked Hollow Fiber Membranes for Natural Gas Purification and Their Manufacture from Novel Polymers, Ph.D. Dissertation, in: Chemical Engineering, The University of Texas at Austin, Austin, TX, 2004.

[7] Qiu, W. L.; Chen, C. C.; Kincer, M. R.; Koros, W. J. Thermal Analysis and Its Application in Evaluation of Fluorinated Polyimide Membranes for Gas Separation. Polymer 2011, 52, 4073.

[8] http://www.chem.wisc.edu/areas/reich/Handouts/nmr-h/hdata.htm

[9] I.C. Omole, S.J. Miller, W.J. Koros, Increased molecular weight of a cross-linkable polyimide for spinning plasticization resistant hollow fiber membranes, Macromolecules, 41 (2008) 6367-6375.

[10] Maurer, J. J.; Eustace, D. J.; Ratcliffe, C. T., Thermal characterization of poly(acrylic acid), Macromolecules 1987, 20, 196–202.

[11] Ho, B. C.; Lee, Y. D.; Chin, W. K. J. Polym. Sci., Part A: Polym. Chem. 1992, 30, 2389–2397.

[12] Mrsevic M,; Düsselberg D,' Staudt C., Synthesis and characterization of a novel carboxyl group containing (co)polyimide with sulfur in the polymer backbone, BEILSTEIN JOURNAL OF ORGANIC CHEMISTRY 2012, 8, 776-786.

[13] Wind, J.D., Improving Polyimide Membrane Resistance to Carbon Dioxide Plasticization in Natural Gas Separations, in *Chemical Engineering*. 2002, The University of Texas at Austin: Austin, Texas. p. 215.

[14] J.H. Kim, W.J. Koros, D.R. Paul, Physical aging of thin 6FDA-based polyimide

membranes containing carboxyl acid groups. Part I. Transport properties, Polymer 47 (2006) 3094–3103

[15] A.M. Kratochvil, THICKNESS DEPENDENT PHYSICAL AGING AND SUPERCRITICAL CARBON DIOXIDE CONDITIONING EFFECTS ON CROSSLINKABLE POLYIMIDE MEMBRANES FOR NATURAL GAS PURIFICATION, PhD Dissertation, in: School of Chemical & Biomolecular Engineering, Georgia Institute of Technology, Atlanta, GA, 2008.

[16] Paris, R,de la Fuente, J. L. J. Polym.Sci. Part B: Polym. Phys. 2007, 45, 1845

[17] Bilyeu, B., Brostow, W., Separation of gelation from vitrification in curing of a fiber-reinforced epoxy composite, Polym Compos. 2002, 23, 1111.

[18] Park, H. B.; Han, S. H.; Jung, C. H.; Lee, Y. M.; Hill, A. J., Thermally rearranged (TR) polymer membranes for CO2 separation, J. Membr. Sci. 2010, 359 (1_2), 11–24.

CHAPTER 6

EFFECTS OF AGGRESSIVE FEED ON HIGH PERFORMANCE ESTER-CROSSLINKED DENSE FILM

6.1 Introduction

In some actual natural gas feeds, feeds can be very aggressive. *Chemically imidized* PDMC and *thermally imidized* PDMC synthesized using optimized condition were characterized under aggressive natural gas feeds. Polyamic acid precursors of *thermally imidized* PDMC were synthesized using the state 6. Effects of high CO_2 partial pressures and operating temperatures were studied with a CO_2/CH_4 mixed gas. The stability of dense films under high feed pressures were also studied.

6.2 Effects of high CO_2 partial pressures

In order to study the CO_2 plasticization suppression at high feed pressure, crosslinked dense films were further characterized by using a 50/50 CO_2/CH_4 mixed gas up to 800 psi of a total feed pressure. Figure 6.1 shows the mixed permeation results of dense films of *chemically imidized* PDMC and *thermally imidized* PDMC crosslinked at 200℃ for 2 hrs.

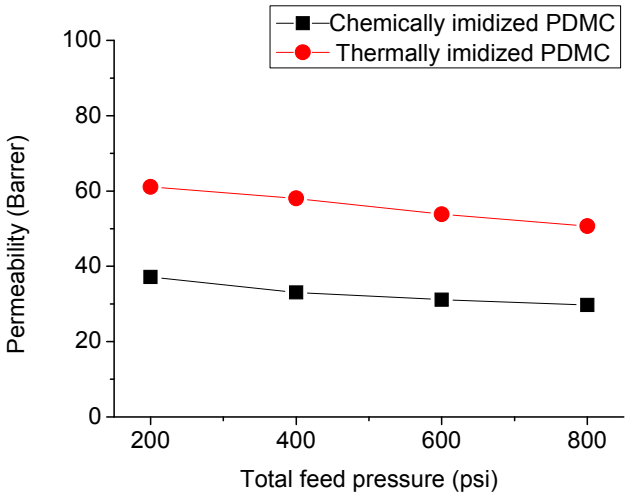

Figure 6.1: CO_2 permeability of crosslinked dense films at elevated feed pressures from this work. Permeability calculated by using fugacity driving force. Test conditions: 50/50 CO_2/CH_4, mixed gas at 35°C.

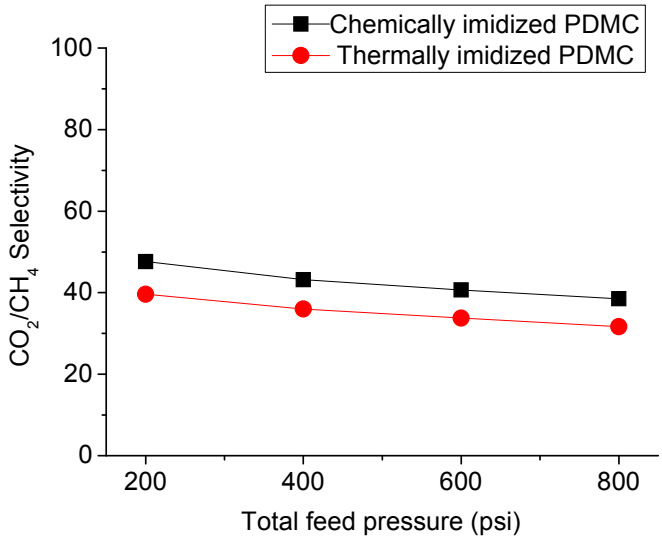

Figure 6.2: CO_2/CH_4 selectivity of crosslinked dense films at elevated feed pressures from this work. Selectivity calculated by using fugacity. Test conditions: 50/50 CO_2/CH_4, mixed gas at 35 °C.

As shown in Figure 6.1, the dense films showed CO_2 permeability over 30 Barrers and 50 Barrers respectively from 200 to 800 psi. Both *chemically imidized* PDMC and *thermally imidized* PDMC showed plasticization suppression up to 800 psi.

As shown in Figure 6.2, the CO_2/CH_4 selectivities ranging from 35 to 40 and from 40 to 50 were attractively high up to 800psi 50/50 CO_2/CH_4 mixed gas at 35℃.

The above permeability and selectivity data showed that both types of PDMC could be applicable in the aggressive feeds.

The downward trends in both permeability and selectivity in the above Figure 6.1 and Figure 6.2 result from dual-mode sorption phenomena as described in Section 2.1.2. [1] As feed pressure Increases, Langmuir saturation increases and the sorption coefficient reduces. These parameter changes result in a decrease of permeability, and the decreased sorption coefficient reduces the ability of carbon

dioxide to out-compete methane for sorption, resulting in a reduction in selectivity with increasing feed pressure. The ability of carbon dioxide to out-compete methane for sorption leads to higher selectivity in mixed gas than in pure gas. In this study, selectivity in mixed gas is approximately 12% higher when comparing mixed gas selectivity (at 700 psi total pressure, 70 psi carbon dioxide partial pressure) to pure gas selectivity (65 psi carbon dioxide pressure).

6.3 Effects of operating temperatures

The *chemically imidized* PDMC and *thermally imidized* PDMC were further characterized at three different operating temperatures 22 °C, 35 °C, and 50 °C to prove consistent performance under aggressive conditions. The CO_2 permeability and CO_2/CH_4 selectivity are depicted in Figure 6.3.

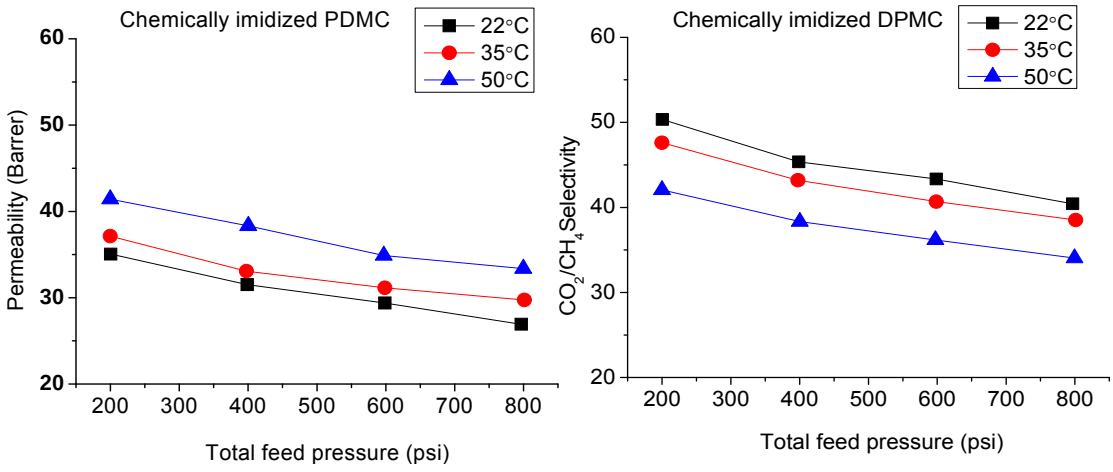

Figure 6.3: Transport properties of crosslinked *chemically imidized* PDMC at different operating temperatures. Transport properties were calculated using fugacity at corresponding temperatures and pressures. Test conditions: 50/50 CO_2/CH_4 mixed gas at 22 ℃, 35 ℃, and 50 ℃ up to total feed 800 psi.

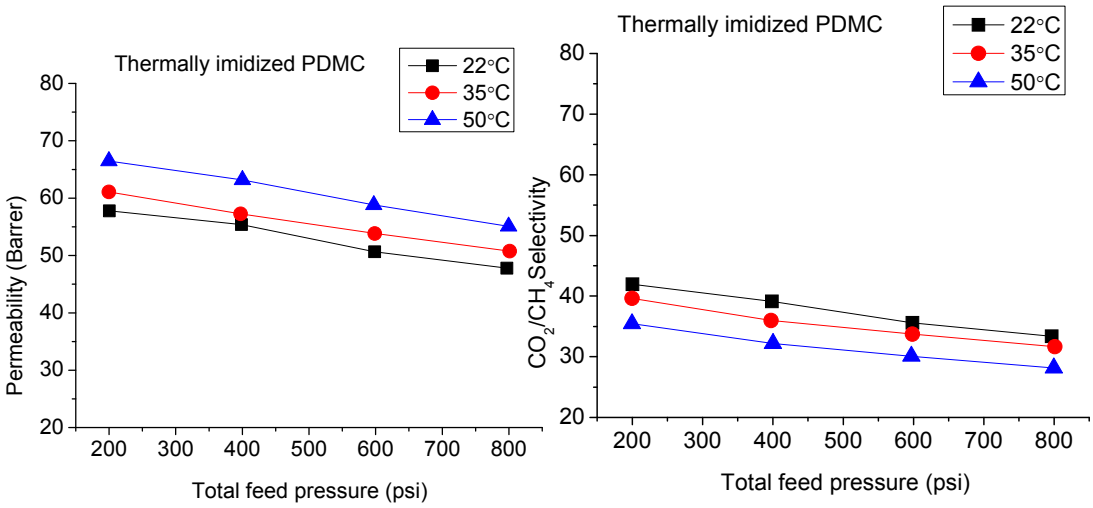

Figure 6.4: Transport properties of crosslinked *thermally imidized* PDMC at different operating temperatures. Transport properties were calculated using fugacity at corresponding temperatures and pressures. Test conditions: 50/50 CO_2/CH_4 mixed gas at 22 ℃, 35 ℃, and 50 ℃ up to total feed 800 psi.

Figure 6.3 and Figure 6.4 show that higher operating temperature can increase the CO_2 permeability and decrease the CO_2/CH_4 selectivity. At high temperature, increased polymer chain mobility increases diffusion coefficients for both CO_2 and CH_4. [2] However, the diffusion coefficient of CH_4 molecule increases faster than that of CO_2 molecule as operation temperature increases. Moreover, the sorption advantage of CO_2 over CH_4 is also reduced as temperature increases. The above two factors causes a loss of CO_2/CH_4 selectivity at higher temperature. Thus, low temperature was preferable for the CO_2/CH_4 separation in terms of selectivity. It is also noteworthy that high operating temperature did not cause CO_2 plasticization up to total feed pressure 800 psi in *thermally imidized* PDMC and chemically imidized PDMC.

The temperature dependence of permeability can be explained by Equation (6.1) [2].

$$P = P_0 exp\left(\frac{-E_p}{RT}\right) \quad (6.1)$$

In this equation, P represents the CO_2 permeability; P_0 is pre-exponential factor; E_p is the activation energy of permeation, and T is the operating temperature. Figure 6.5 was obtained by plotting log P vs. 1000/T.

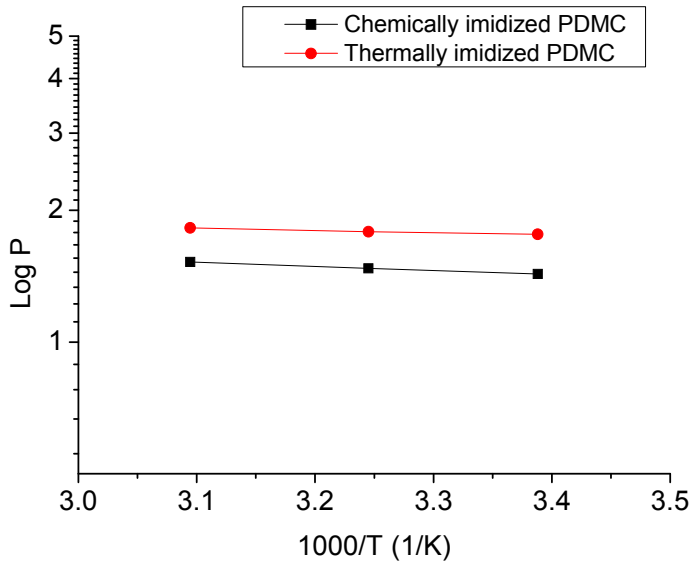

Figure 6.5: Plotting log P vs. 1000/T.

Figure 6.5 suggests that there exists a good linearity between log P and 1000/T for CO_2 permeability at 800psi for both *chemically imidized* PDMC and *thermally imidized* PDMC (R^2 = 0.999, R^2 = 0.864 respectively). This also means that Equation 9 fits the permeability data measured in this study.

6.4 Stability of dense films under high feed pressures

As discussed in section 6.3, the dense films both *chemically imidized* PDMC and *thermally imidized* PDMC showed sufficient separation productivity with high selectivity under a total feed pressure up to 800 psi of 50/50 CO_2/CH_4 mixed gas. Despite this high performance, to simulate realistic operation conditions, it is crucial to investigate effects of exposure of dense films under a high feed pressure for a long period of time before proceeding to application of hollow fibers. The crosslinked dense films were tested by using 600 psi of a 50/50 CO_2/CH_4 mixed gas at 35 ℃. Every 24hours, separation performance was measured every 24 hours until 96 hours. The permeation results are shown in Figure 6.6.

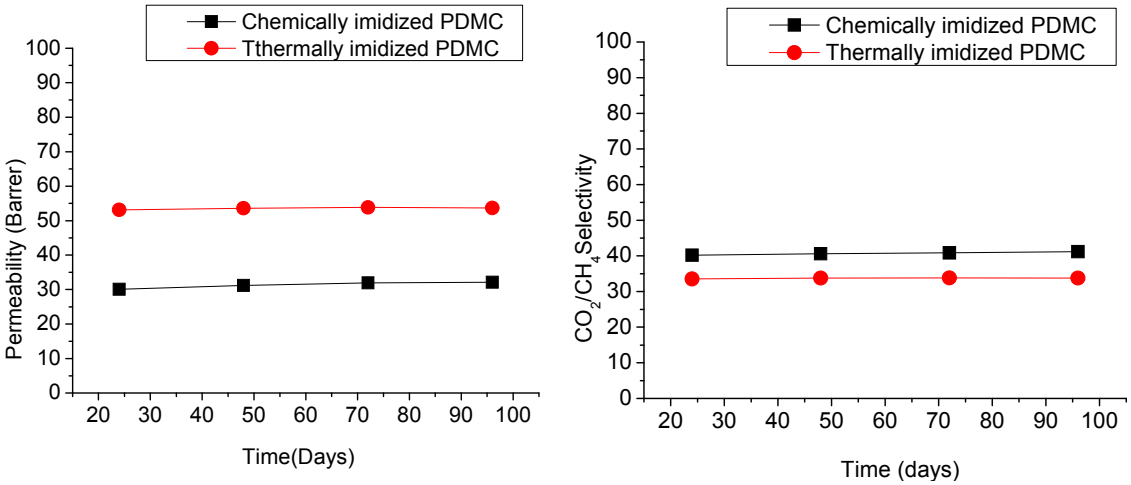

Figure 6.6: Stability of crosslinked dense films under high feed pressures. Permeabilities and selectivities were calculated using fugacity driving force at corresponding temperatures and pressures. Test conditions: 600 psi, 50/50 CO_2/CH_4 mixed gas at 35 ℃.

In Figure 6.6, both *chemically imidized* PDMC and *thermally imidized* PDMC showed a stable permeability and selectivity. This indicates that the ester-crosslinked dense films are ready to proceed to fiber application in the realistic operation environment. If dense films were exposed in air, permeability may decrease and

selectivity may increase due to aging of the films; however, the effects of aging are more extreme for fibers. Aging occurs from so called relaxation of free volume [3]. However, exposure of dense films under CO_2 feed pressure prevents relaxation of the free volume inside polymer by occupation of CO_2 molecules inside the free volume, thereby keeping transport properties constant. Therefore, we anticipate that physical aging will e of secondary importance even in actual asymmetric fibers. Nevertheless, this must be verified.

6.5 Conclusions

Chemically imidized PDMC and thermally imidized PDMC showed good plasticization suppression up to total feed pressure 800psi of 50/50 CO_2/CH_4 mixed gas at 35°C. Operating temperatures were also studied, and showed that as temperature increases, permeability decreases and selectivity increases. Relatively thick dense films compared to hollow fibers showed sufficient stability under high feed pressures for 96 hours.

6.6 References

[1] Chern, R. T., Koros, W. J., Sanders, E. S.; Yui, R, IMPLICATIONS OF THE DUAL-MODE SORPTION AND TRANSPORT MODELS FOR MIXED GAS PERMEATION, J Membr Sci 1983, 15, 157–169.

[2] T.S. Chung, C. Cao, R. Wang, Pressure and temperature dependence of the gas-transport properties of dense poly[2,6-toluene-2,2-bis(3,4dicarboxylphenyl)hexafluoropropane diimide] membranes, J Polym Sci Pol Phys, 42 (2004) 354-364.

[3] A.M. Kratochvil, THICKNESS DEPENDENT PHYSICAL AGING AND SUPERCRITICAL CARBON DIOXIDE CONDITIONING EFFECTS ON CROSSLINKABLE POLYIMIDE MEMBRANES FOR NATURAL GAS PURIFICATION, PhD Dissertation, in: School of Chemical & Biomolecular Engineering, Georgia Institute of Technology, Atlanta, GA, 2008.

CHAPTER 7

CONCLUSION AND RECOMMENDATION FOR FUTURE WORK

7.1 Summary

This research addresses the fundamental understanding of effects of polymerization conditions and imidization methods on polymer properties of *chemically imidized* PDMC, and characterization of *thermally imidized* PDMC and *chemically imidized* PDMC. The work showed the critical importance of controlling the various phases of formation, beginning with the actual polymerization and ending with the final crosslinking processes.

7.2 Conclusions

7.2.1 Optimization of polymerization conditions of *chemically imidized* PDMC

The state polymerized at 5℃ for 72 hours showed the best selectivity. Most states showed selectivity 33~37 and showed permeability 38~43, except the states 1, 4, and 7 polymerized for insufficient time. Transport properties difference was small. Given moderately low temperature (0 ℃~5 ℃) and sufficient polymerization time (48 hours~72 hours), molecular weight and transport properties of states are expected to be similar to each other.

7.2.2 Significantly improved separation performance of *thermally imidized* PDMC

Thermally imidized PDMC showed 70% higher permeability without major selectivity losses compared to *chemically imidized* PDMC. According to our working hypothesis, high temperature ~190 ℃ of thermal imidization renders the monomer sequence more randomized. DSC, DMA, and XRD supported this concept of randomized monomer sequence in *thermally imidized* PDMC. Other possibilities,

which may explain the permeability difference between *chemically imidized* PDMC and *thermally imidized* PDMC, were ruled out by FTIR, TGA, NMR.

7.2.3 Characterization of ester-crosslinked dense film under aggressive gas feed

Both *chemically imidized* PDMC and *thermally imidized* PDMC showed consistent and adequate separation performance under aggressive gas feed. Particularly, in order to simulate the real gas feed, 50/50 CO_2/CH_4 mixed gas was adopted. Both PDMC showed plasticization suppression up to 800 psi of 50/50 CO_2/CH_4 at 35 ℃. Separation performance of both PDMC at fairly high temperature 50 ℃ was still within the attractive region. In addition, both PDMC showed good stability under high feed pressures during 120 hours.

7.3 Recommendations for Future Work

7.3.1 Sorption test on *chemically imidized* PDMC and *thermally imidized* PDMC

As shown in earlier sections, separation performance of *chemically imidized* PDMC and *thermally imidized* PDMC differs. Further study of sorption and diffusion for both PDMC type samples may clarify the basis for the different permeation behavior. Specifically, comparison of the magnitude of the Langmuir's mode, Henry's mode, and the associated diffusion coefficients for penetrant will add insight into the difference between the two PDMC samples.

7.3.2 Extension to composite hollow fiber

Using *chemically imidized* PDMC and *thermally imidized* PDMC synthesized in this work, PDMC/Torlon, PDMC/P84, and PDMC/Cellulose acetate composite hollow fibers can be spun. Torlon, P84 and cellulose acetate will be studied as high performance core layer materials. Ma did preliminary work on PDMC/Torlon and PDMC/Cellulose acetate composite hollow fibers [1]. Ma proved attractive separation performance of ester-crosslinked PDMC/Torlon composite hollow fibers with sufficient

chemical stability. However, skin layer thickness has not been optimized to obtain the best permeability of composite hollow fiber. In case of PDMC/Cellulose acetate composite hollow fibers, cellulose acetate core layer was collapsed during crosslinking at 200 ℃. The collapse is mainly caused by cellulose acetate's low glass transition temperature which is 180 ℃~210 ℃.

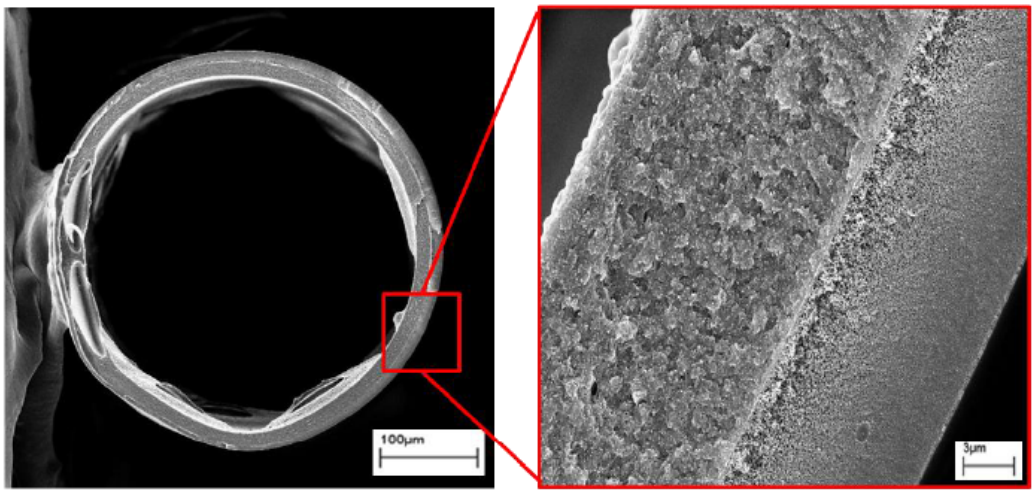

Figure 7.1: Scanning electron microscope (SEM) images showing the cross-section of a crosslinked PDMC/CA composite hollow fiber [1].

The crosslinking temperature should be lowered to below 180℃ to explore the use of cellulose acetate as the core layer. If the crosslinking temperature for monolithic fibers can be reduced to below 180 ℃, composite hollow fibers using *chemically imidized* PDMC and *thermally imidized* PDMC will be formed and characterized. We hypothesize that *thermally imidized* PDMC, which we believe has more randomized monomer sequence, will show better adhesion to core cellulose acetate layer because of more distributed ester bonds.

7.3.3 Aggressive feed conditions

The high performance ester-crosslinked dense film membranes in this work

were characterized by using a 50/50 CO_2/CH_4 mixed gas with or without contaminants. In the future work, further mixed gas permeation can be done with a high CO_2 concentration over 50% in the feed to investigate plasticization suppression of composite hollow fibers under higher CO_2 partial pressure. Moreover, other impurities such as toluene, heptane, water, and H_2S could exist in the practical gas feeds [2]. The separation performance of crosslinked composite hollow fiber under those aggressive feed conditions should be explored.

7.4 References

[1] C. Ma, Highly Productive Ester Crosslinkable Composite Hollow Fiber Membranes for Aggressive Natural Gas Separations, Ph.D. Dissertation, in: School of Chemical and Biomolecular Engineering, Georgia Institute of Technology, Atlanta, GA, 2011.

[2] I.C. Omole, Crosslinked Polyimide Hollow Fiber Membranes for Aggressive Natural Gas Feed Streams, Ph.D. Dissertation, in: Chemical and Biomolecular Engineering, Georgia Institute of Technology, Atlanta, GA, 2008.

Appendix A: CHEMICAL IMIDIZATION

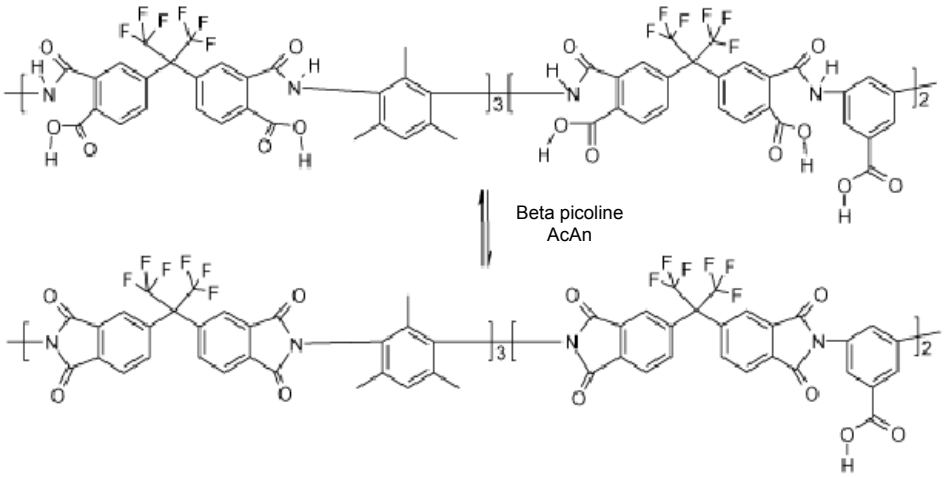

Figure A.1: Chemical imidization reaction of polyamic acid with beta picoline and acetate anhydride below room temperature [1].

1) Add NMP in the flask filled with precipitated 6FDA-DAM-DABA.

2) Add beta picoline via syringe.

3) Add Acetic Anhydride at this stage via addition funnel slowly.

4) Let this solution react for about 22 hours below room temperature with purging.

5) Pour the polyimide solution in a beaker with methanol with continuous stirring.

6) Blend, filter, and wash the polymer with methanol.

7) Dry it under the hood overnight.

8) Dry the polymer in the vacuum oven at 210 ℃ for 12 hours.

Appendix B: THERMAL IMIDIZATION

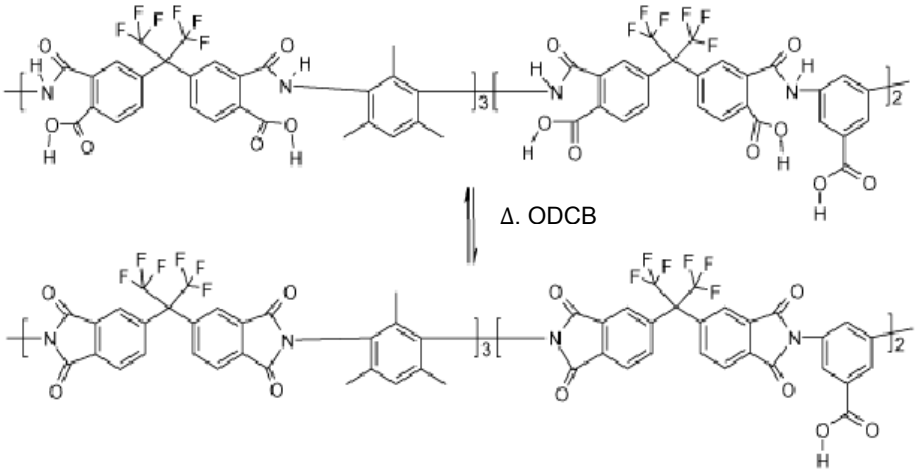

Figure B.1: Thermal imidization reaction of polyamic acid with ODCB at 190 ℃ [1].

1) Add 2.5 mL of ortho-dichlorobenzene (ODCB) per gram polyimide to reaction solution.

2) Increase the temperature of 6FDA-DAM-DABA solution up to 190 ℃.

3) Let this solution react for about 22 hours at 190 ℃.

4) If you plan to do monoesterification, proceed to do monoesterification in “one pot”.

Appendix C: MONOESTERIFICATION

The 6FDA-DAM: DABA (3:2) precursor is monoesterified with 1, 3-propanediol. The reaction mechanism is shown in Figure C.1.

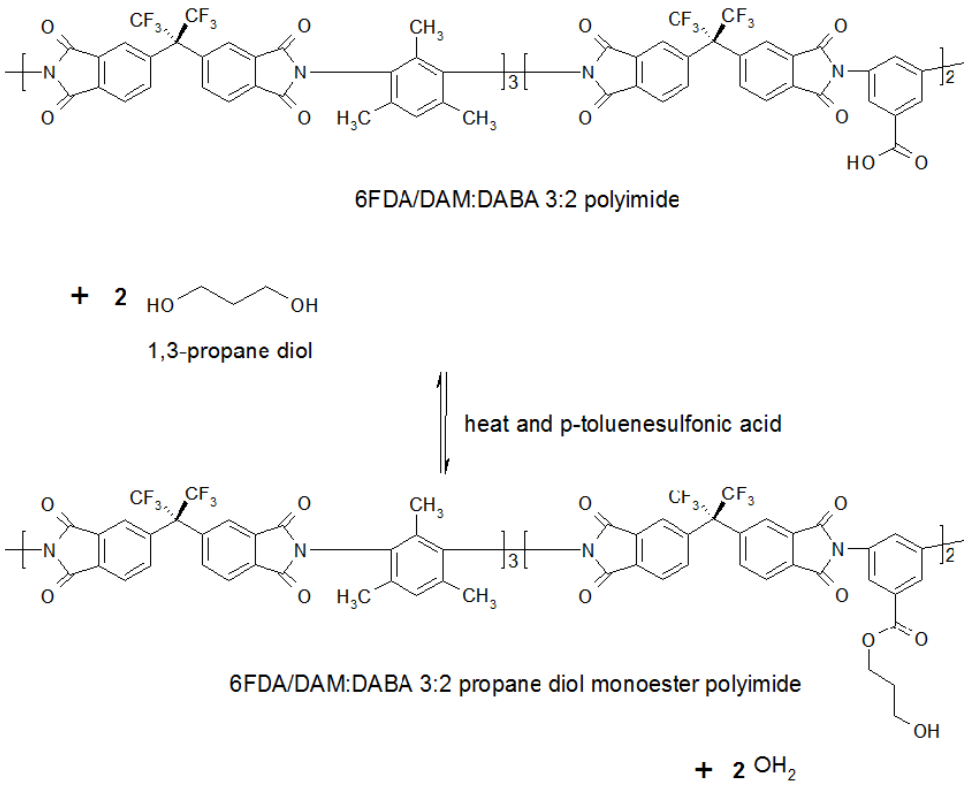

Figure C.1: Monoesterification reaction of 6FDA-DAM: DABA (3:2) polyimide with 1,3-propanediol [1].

The monoesterification reaction is conducted by the following procedures:

1) Dry molecular sieves to dry NMP, dehydrating agents and 1,3-propanediol.

2) Clean and dry glassware.

3) Needle-transfer NMP to round-bottom flask filled with molecular sieves.

4) Transfer ortho-dichlorobenzene (ODCB) to round-bottom flask filled with molecular sieves.

5) Transfer 1,3-propanediol to round-bottom flask filled with molecular sieves.

6) Assemble glassware in fume hood, as shown in Figure C.2.

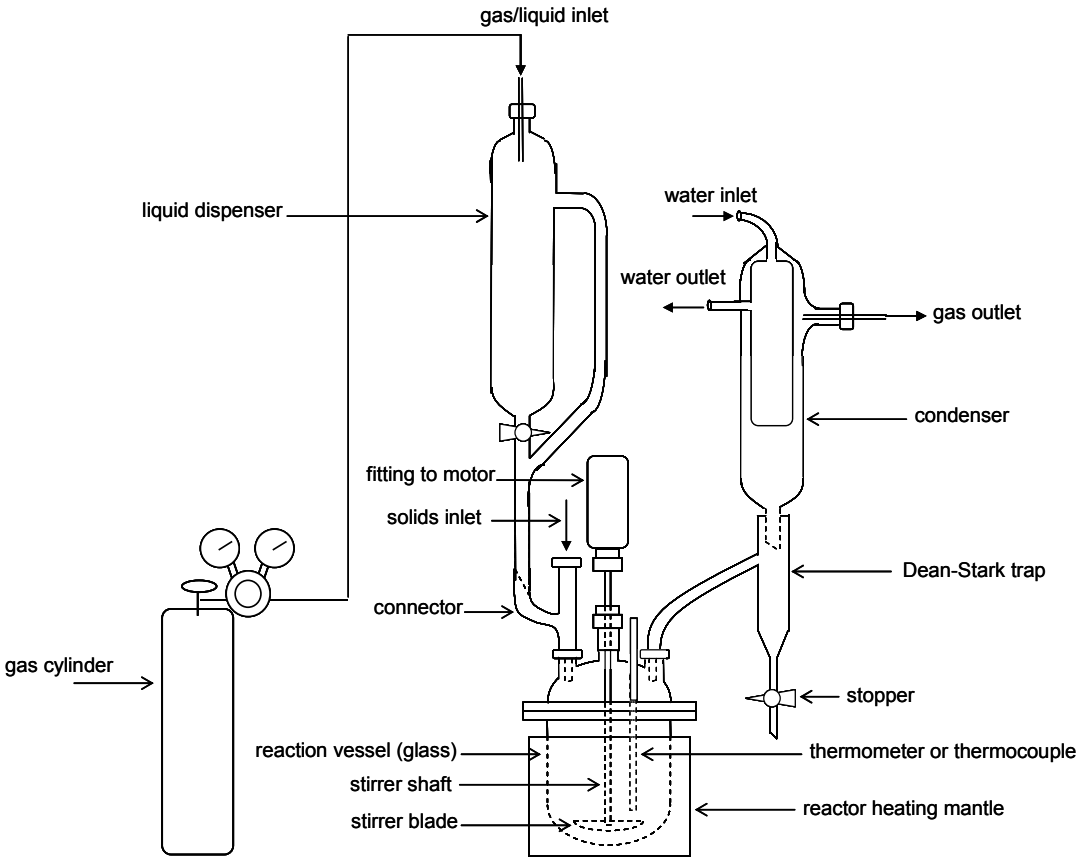

Figure C.2: Schematic showing the set-up for monoesterification reaction [1].

7) Weigh the 6FDA-DAM: DABA (3:2) polyimide precisely.

8) Dissolve the 6FDA-DAM: DABA (3:2) polyimide in NMP with a polymer content of 20wt % in the flask.

9) Heat up the solution to ~140 ℃ and keep purging the reaction with N_2 gas.

10) Add 2.5 mL of ortho-dichlorobenzene (ODCB) per gram polyimide to reaction solution.

11) Add 2.5 mg of para-toluenesulfonic acid (p-TSA) per gram polyimide to solution.

12) Add 40 to 70 times the stoichiometric amount of 1, 3-propanediol slowly to avoid forming large precipitates.

13) React for 24 hours at 130 ℃ while collecting water produced.

14) Cool reaction solution to less than 70 ℃ and precipitate solution by pouring solution slowly into methanol solvent.

15) Blend polymer, wash several times with methanol, filter, and dry in hood overnight.

16) Dry polymer in vacuum oven at 70 ℃ for 24 hours to evaporate methanol.

References

[1] C. Ma, OPTIMIZATION OF ASYMMETRIC HOLLOW FIBER MEMBRANES FOR NATURAL GAS SEPARATION, MS THESIS, in: School of Chemical and Biomolecular Engineering, Georgia Institute of Technology, Atlanta, GA, 2011.

[2] I.C. Omole, Crosslinked Polyimide Hollow Fiber Membranes for Aggressive Natural Gas Feed Streams, Ph.D. Dissertation, in: Chemical and Biomolecular Engineering, Georgia Institute of Technology, Atlanta, GA, 2008.